The Chern-Simons current in systems of DNA-RNA transcriptions

Salvatore Capozziello

Nonlinearity, Nonlocality, and Ultrametricity
Belgrade, May 26-30, 2025

SSM
Scuola Superiore Meridionale

Summary

A **Chern-Simons current**, coming from ghost and anti-ghost fields of supersymmetry theory, can be used to define a **spectrum of gene expression** in new time series data where a **spinor field**, as alternative representation of a gene, is adopted **instead of using the standard alphabet sequence of bases A,T,C,G,U.** We give examples of the use of **supersymmetry for living organisms**, discuss the codon and anti-codon ghost fields and develop an **algebraic construction** for **trash DNA**, the DNA area which does not seem active in biological systems. As a general result, **all hidden states of codon can be computed by Chern-Simons 3 forms**. Finally, we plot a time series of genetic variations of viral glycoprotein gene and host T-cell receptor gene by using a gene tensor correlation network related to the Chern- Simons current. An empirical analysis of genetic shift, in host cell receptor genes with separated cluster of gene and genetic drift in viral gene, is obtained by using a tensor correlation plot over time series data derived as the empirical mode decomposition of Chern-Simons current.

In collaboration with

Prof. Carlo Altucci
University of Naples
“Federico II”
Naples - Italy

Dr. Francesco Bajardi
Scuola Superiore
Meridionale, Naples -
Italy

Dr. Erik Bartos
Slovak Academy of
Sciences
Watsonova -
Slovakia

Dr. Richard Pincak
Slovak Academy of
Sciences
Watsonova - Slovakia

Prof. Emmanuel Saridakis
National Observatory of
Athens, Greece

Plan of the presentation:

- *Preliminaries*
  - *Successes and shortcomings of Einstein's General Relativity*
  - *Extended gravity and topological field theories*

- *Application of Chern-Simons theory:*
  - Cosmological Background
  - Spherically Symmetric Background
  - Three-dimensional electromagnetism

- *Application to Biological Systems*
  - Foundation and theoretical structure
  - Application to KRAS human Gene
  - Application to Sars-COV-2

- *Conclusions and perspectives*

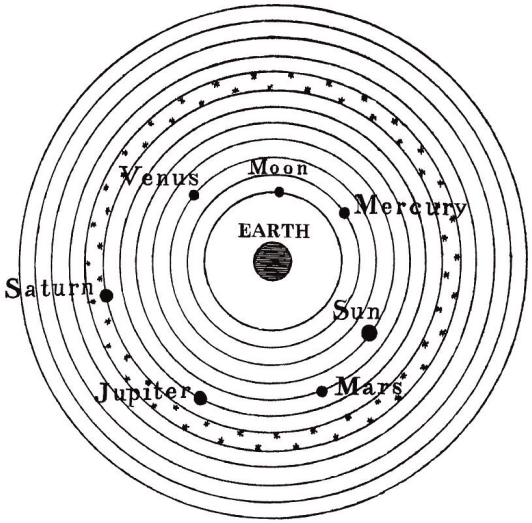

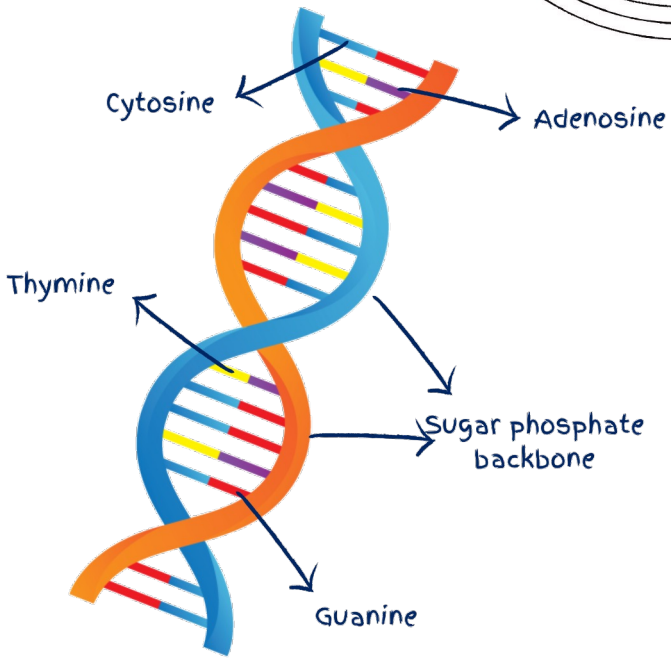

General Relativity: Successes

$$R_{\mu\nu} - \frac{1}{2} g_{\mu\nu} R = 8\pi G \mathcal{T}_{\mu\nu}$$

Modern Cosmology

Gravitational Waves

Black holes

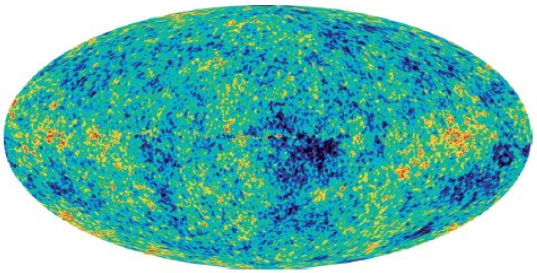

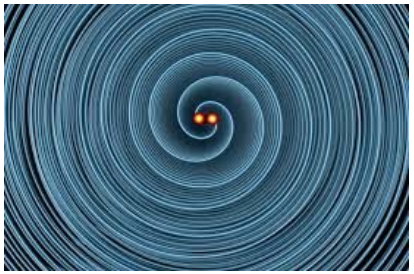

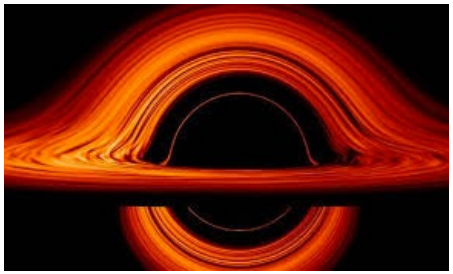

$$ds^2 = dt^2 - a(t)^2 \delta_{ij} dx^i dx^j$$

$$g_{\mu\nu} = \eta_{\mu\nu} + h_{\mu\nu}$$

$$ds^2 = e^{\nu(r,t)} c^2 dt^2 - e^{\lambda(r,t)} dr^2 - r^2(\sin^2\theta d\phi^2 + d\theta^2).$$

General Relativity shortcomings

Large Scales

- Universe accelerating expansion
- Inflation

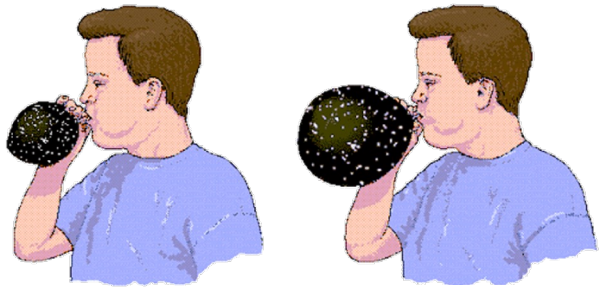

$$R_{\mu\nu} - \frac{1}{2} g_{\mu\nu} R + \Lambda g_{\mu\nu} = 8\pi G \mathcal{T}_{\mu\nu}$$

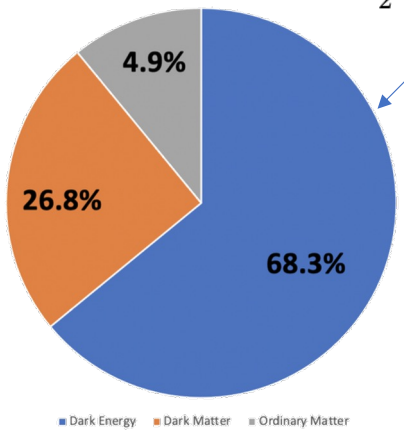

- Galaxy Rotation Curve

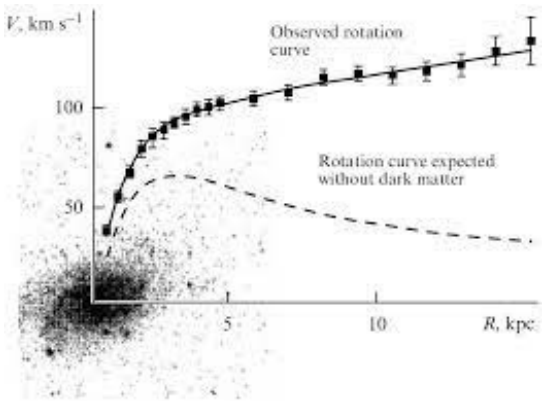

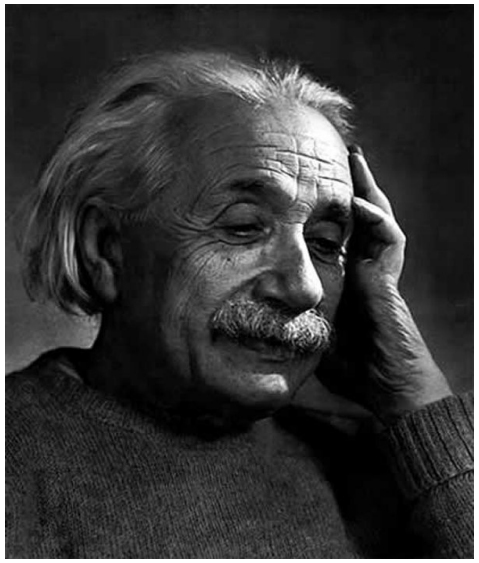

- Mass-Radius diagram of neutron stars

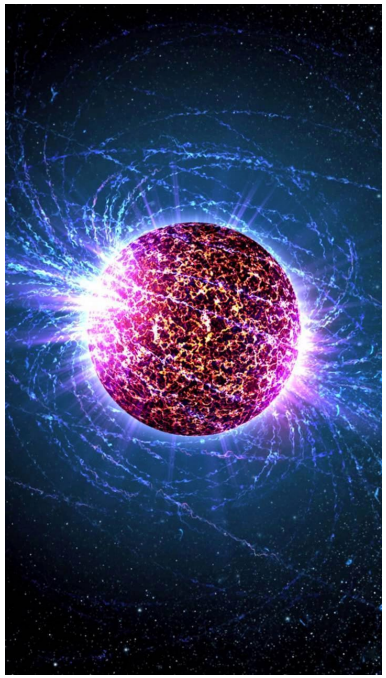

General Relativity shortcomings

Small Scales

➢Renormalization
➢Quantization

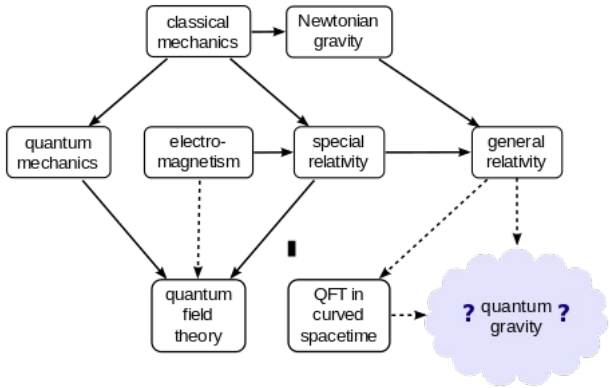

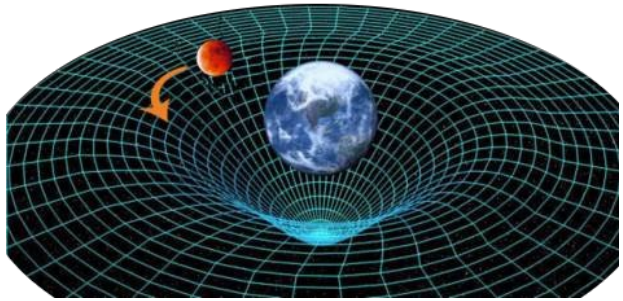

➢Discrepancy between theoretical and experimental Λ

$$R_{\mu\nu} - \frac{1}{2} g_{\mu\nu} R + \Lambda g_{\mu\nu} = 8\pi G \mathcal{T}_{\mu\nu}$$

$$\frac{\rho'_\Lambda}{\rho_\Lambda} = \frac{\hbar^2}{96\pi^3 G H_0^2} \sim 10^{121}$$

➢Cannot be treated using the same formalism of QFT

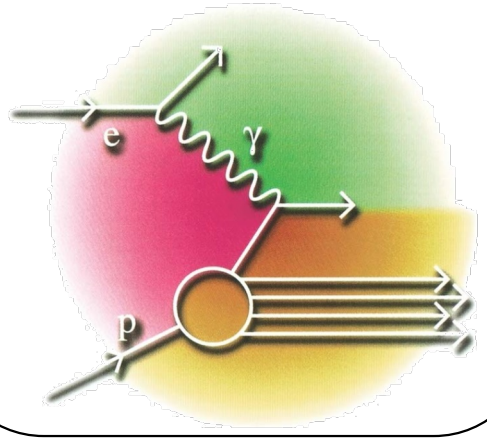

➢Space-time singularity

Unfortunately, thus far, no theory is able to solve all these problems at once!

Modified theories of gravity

Extended theories of gravity

$$S = \int \sqrt{-g} f(R)\, d^4x.$$

Alternative theories of gravity

$$\Gamma^{\alpha}_{[\mu\nu]} \neq 0$$

Topological Field Theories

Chern-Simons Theory

$$L = L\left(g_{ab}, R_{abcd}, \nabla_{a_1} R_{bcde}, \ldots, \nabla_{a_1 \ldots a_p} R_{bcde}\right)$$

Topological Invariants

Depend on the topology, independently of the space-time geometry

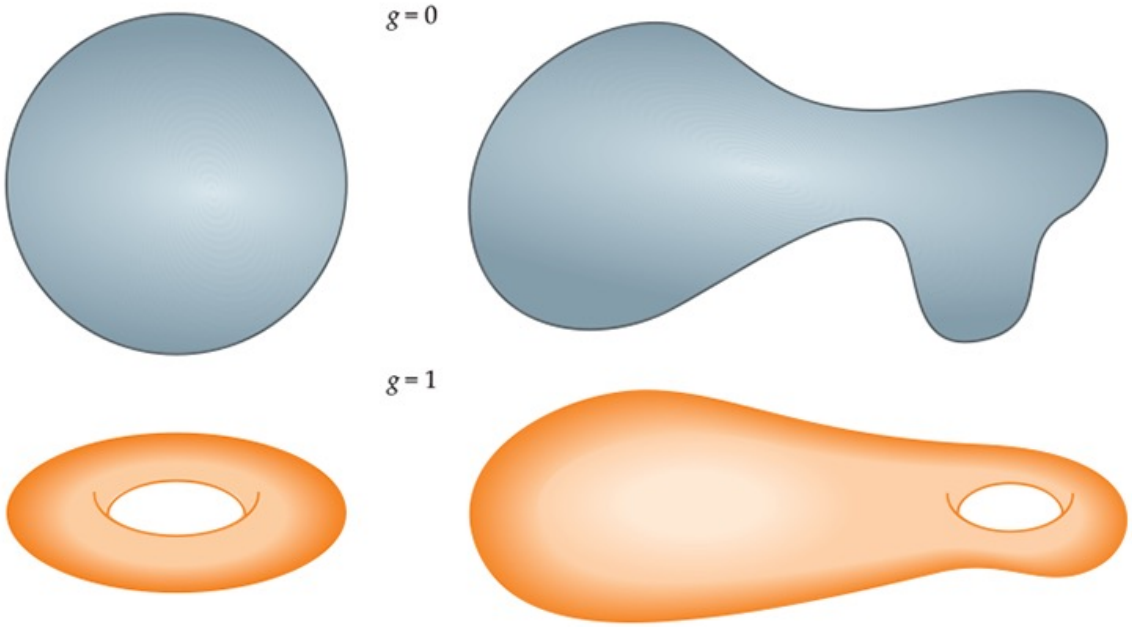

$$\frac{1}{2\pi}\int K\,dA = 2(g-1)$$

Torus cannot be obtained by deforming the sphere

They do not depend on the local form of the spacetime, but only relies on its global structure

Lovelock and Chern-Simons theories

Lovelock action

$$S = \kappa \int_{\mathcal{M}} \sum_{i=0}^{\frac{D}{2}} \alpha_i \mathscr{L}^{(D,i)}$$

$$\mathscr{L}^{(D,i)} = \epsilon_{a_1,a_2 \ldots a_D} R^{a_1 a_2} \wedge R^{a_3 a_4} \wedge \ldots \wedge R^{a_{2i-1} a_{2i}} \wedge e^{a_{2i+1}} \wedge e^{a_{2i+2}} \wedge \ldots \wedge e^{a_D}$$

$SO(1, D-1)$

It is the most general action ***without torsion*** which leads to ***second-order field equations***

*The **GB** term naturally emerges* →

$$\mathcal{G} = \epsilon_{a_1,a_2,a_3 \ldots . a_n} R^{a_1,a_2} \wedge R^{a_3,a_4} \wedge e^{a_5} \wedge \ldots \wedge e^{a_n}$$

Four-dimensional limit

$$S = \kappa \int \sqrt{-g} \left(\alpha_0 + \alpha_1 R + \alpha_2 \mathcal{G}\right) d^4x$$

$$\mathscr{L}^{(4)} = \epsilon_{abcd} \left[\alpha_2 R^{ab} \wedge R^{cd} + \alpha_1 R^{ab} \wedge e^c \wedge e^d + \alpha_0 e^a \wedge e^a \wedge e^b \wedge e^c \wedge e^d\right]$$

Topological surface → It follows that →

Lovelock Theorem:

The H-E action is the most general four-dimensional action leading to second-order field equations

J. Zanelli. arXiv:hep-th/0502193

Chern-Simons theory

Starting from Lovelock action, it is possible to select the coefficients such that the resulting theory is invariant with respect to some gauge group

$$S = \kappa \int_{\mathcal{M}} \sum_{i=0}^{\frac{D}{2}} \alpha_i \mathscr{L}^{(D,i)}$$

Proceed by trial and error

Find a methodical procedure → **All D-dimensional Lagrangians whose exterior derivative provides a topological surface term, are *quasi* gauge-invariant** $E = d\mathcal{L}$.

Why Chern-Simons?

- It fits the formalism of QFT
- It can be quantized
- It can be applied to SUGRA
- It can be renormalized
- AdS/CFT correspondence

Shiing-Shen Chern

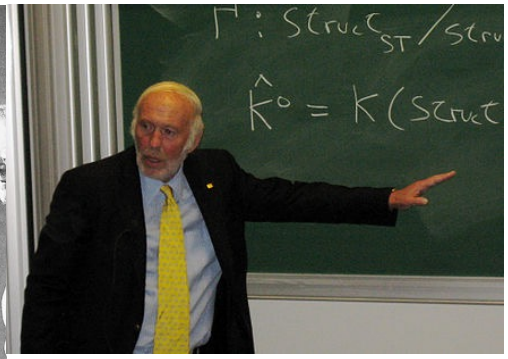

James Harris Simons

Chern-Simons Lagrangians

$D=3$ Chern-Simons Lagrangian	Top. Invariant($\mathcal{P}$)	Group
$L_3^{(A)dS} = \epsilon_{abc}(R^{ab} \pm \frac{e^a e^b}{3l^2})e^c$	$E_4 = \epsilon_{abc}(R^{ab} \pm \frac{e^a e^b}{l^2})T^c$	$SO(4)\dagger$
$L_3^{Lorentz} = \omega^a{}_b d\omega^b{}_a + \frac{2}{3}\omega^a{}_b\omega^b{}_c\omega^c{}_a$	$P_4^{Lorentz} = R^a{}_b R^b{}_a$	$SO(2,1)$
$L_3^{Torsion} = e^a T_a$	$N_4 = T^a T_a - e^a e^b R_{ab}$	$SO(2,1)$
$L_3^{U(1)} = AdA$	$P_4^{U(N)} = FF$	$U(1)$
$L_3^{SU(N)} = tr[\mathbf{A}d\mathbf{A} + \frac{2}{3}\mathbf{AAA}]$	$P_4^{SU(4)} = tr[\mathbf{FF}]$	$SU(N)$

*Examples of three-dimensional **CS** Lagrangians*

Chern-Simons theory: three possible applications

$\mathscr{L} = AdA$ → U(1) invariant

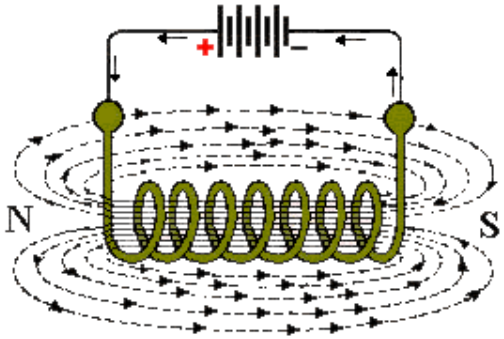

Related topological surface

Electromagnetism ← $P_4^{U(N)} = dAdA$

$\mathscr{L} = \mathrm{Tr}\left(\mathbf{A} \wedge d\mathbf{A} + \frac{2}{3}\mathbf{A} \wedge \mathbf{A} \wedge \mathbf{A}\right)$ → SU(N) invariant

Related topological surface

Biological systems ← $P_4^{SU(4)} = Tr[dAdA]$

$\mathscr{L}_5^{AdS} = \frac{1}{\ell}\epsilon_{abcde}\left(R^{ab} \wedge R^{cd} \wedge e^e + \frac{2}{3\ell^2}R^{ab} \wedge e^c \wedge e^d \wedge e^e + \frac{1}{5\ell^4}e^a \wedge e^b \wedge e^c \wedge e^d \wedge e^e\right)$ → AdS invariant

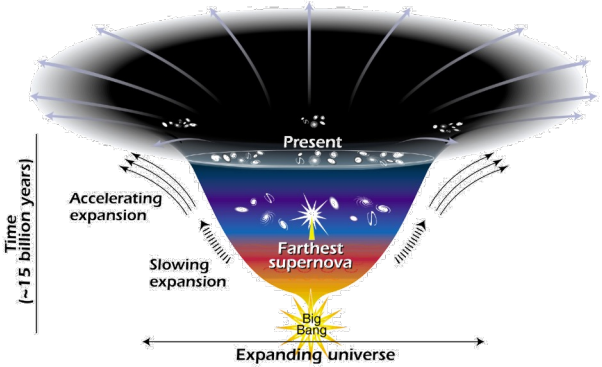

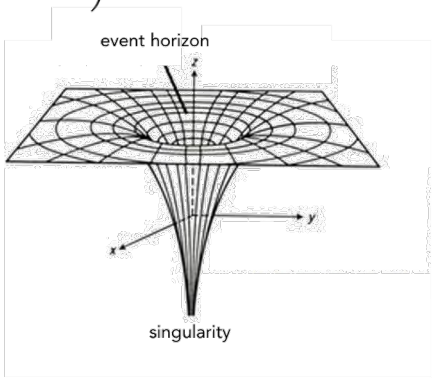

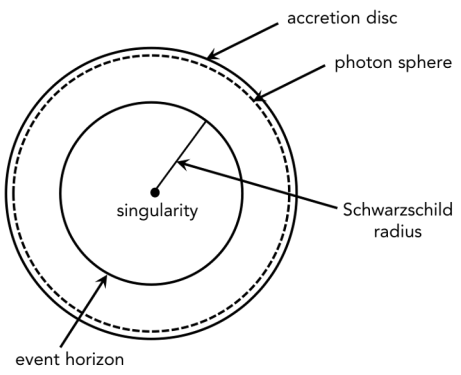

Related topological surface

Cosmology and Black holes ← $E_6 = 2R^{abcd}R_{cdef}R_{ab}^{ef} + 8R_{cd}^{ab}R_{bf}^{ce}R_{ae}^{df} + 24R^{abcd}R_{cdbe}R_a^e + 3RR^{abcd}R_{abcd}$

$+24R^{abcd}R_{ac}R_{bd} + 16R^{ab}R_{bc}R_a^c - 12RR^{ab}R_{ab} + R^3$.

Cosmological applications

$$ds^2 = dt^2 - \frac{a(t)^2}{1-kr^2}dr^2 - r^2 d\Omega^2_{d-1}$$

$$S = \kappa \int |e| \left[\alpha_0 + \alpha_1 \mathcal{R}^{(d+1)} + \alpha_2 \mathcal{G}^{(d+1)}\right] d^{d+1}x$$

Starting line element and starting action

d+1 dimensional expression of scalar curvature and GB term

$$\mathcal{R}^{(d+1)} = -d\left[2\frac{\ddot{a}}{a} + (d-1)\left(\frac{\dot{a}^2+k}{a^2}\right)\right]$$

$$\mathcal{G}^{(d+1)} = d(d-1)(d-2)\left[(d-3)\left(\frac{\dot{a}^4}{a^4} + 2k\frac{\dot{a}^2}{a^4} + \frac{k^2}{a^4}\right) + \frac{4}{3a^3}\frac{d}{dt}\left(\dot{a}^3\right) + 4k\frac{\ddot{a}}{a^3}\right]$$

$$\mathcal{L} = \frac{r^{d-2}a^{d-4}}{3\sqrt{1-kr^2}} \left\{3a^2[a^2\alpha_0 + \alpha_1 d(d-1)(\dot{a}^2-k)] - \alpha_2 d(d-1)(d-2)(d-3)(\dot{a}^4 + 6k\dot{a}^2 - 3k^2)\right\}$$

Cosmological Lagrangian

F. Bajardi, D. Vernieri, S. Capozziello, "Exact solutions in higher-dimensional Lovelock and AdS5 Chern-Simons gravity," 10.1088/1475-7516/2021/11/057

Case	α_0	α_1	α_2	k	Scale Factor	Dimension
Einstein–de Sitter	$\neq 0$	$\neq 0$	0	$\neq 0$	$a(t) = \pm\sqrt{\frac{\alpha_1 k\, d(d-1)}{\alpha_0 - \alpha_0 \coth^2\left[\sqrt{\alpha_0}\left(c_1 + \frac{t}{\sqrt{\alpha_1(d-1)d}}\right)\right]}}$	Any
				0	$a(t) = a_0 e^{\pm\sqrt{\frac{\alpha_0}{\alpha_1 d(d-1)}}\,t}$	
					$a(t) = a_0 e^{\pm\sqrt{\frac{\alpha_0}{12\alpha_1}}\,t}$	5
Pure Gauss–Bonnet	$\neq 0$	0	$\neq 0$	0	$a(t) = a_0 \exp\left\{\pm\sqrt[4]{\frac{-\alpha_0}{d(d-1)(d-2)(d-3)\alpha_2}}\,t\right\}$ $a(t) = b(t)$	Any
					$a(t) = a_0 \exp\left\{\pm\sqrt[4]{\frac{-\alpha_0}{24\alpha_2}}\,t\right\}$	5
	0	0	$\neq 0$	$\neq 0$	$a(t) = \sqrt{-k}\,t$	Any
				0	$a(t) \sim$ Const.	
					$a(t) \sim$ Const.	5
Lovelock	$\neq 0$	$\neq 0$	$\neq 0$	0	$a(t) = a_0 \exp\left\{\pm\sqrt{\frac{2\alpha_0}{\pm\sqrt{(d-1)d\,[\alpha_1^2(d-1)d - 4\alpha_0\alpha_2(d-3)(d-2)]} + \alpha_1 d(d-1)}}\,t\right\}$	Any
					$a(t) = a_0 \exp\left\{\pm\sqrt{\frac{\alpha_0}{\pm 2\sqrt{9\alpha_1^2 - 6\alpha_0\alpha_2} + 6\alpha_1}}\,t\right\}$	5
	0	$\neq 0$	$\neq 0$	$\neq 0$	$a(t) = \pm\sqrt{\frac{-\alpha_2 k(d-3)(d-2)}{\alpha_1}}\sinh\left[\sqrt{\alpha_1}\left(\frac{t}{\sqrt{\alpha_2(d-3)(d-2)}} + c_1\right)\right]$	Any
				0	$a(t) = a_0 \exp\left\{\pm\sqrt{\frac{\alpha_1}{\alpha_2\,(d-2)\,(d-3)}}\,t\right\}$	
					$a(t) = a_0 \exp\left\{\pm\sqrt{\frac{\alpha_1}{2\alpha_2}}\,t\right\}$	5
Chern–Simons	$\frac{1}{5l^4}$	$\frac{2}{3l^2}$	1	0	$a(t) = a_0 \exp\left\{\pm\frac{1}{l}\sqrt{\frac{1}{6}\left(1 \pm \sqrt{\frac{7}{10}}\right)}\,t\right\}$	

Spherical symmetry

$$ds^2 = P(r)^2 dt^2 - Q(r)^2 dr^2 - r^2 d\Omega_{d-1}^2$$

$$S = \kappa \int |e| \left[\alpha_0 + \alpha_1 \mathcal{R}^{(d+1)} + \alpha_2 \mathcal{G}^{(d+1)}\right] d^{d+1}x$$

Starting line element and starting action

d+1 dimensional expression of scalar curvature and GB term

$$\mathcal{R}^{(d+1)} = \frac{2r\left\{Q\left[(d-1)P' + rP''\right] - rP'Q'\right\} + (1-d)P\left[(d-2)Q^3 + (2-d)Q + 2rQ'\right]}{r^2 P Q^3}$$

$$\mathcal{G}^{(d+1)} = \frac{(d-2)(d-1)}{r^4 P Q^5}\Big\{(d-3)P\left(Q^2-1\right)\left[(d-4)Q^3 - (d-4)Q + 4rQ'\right] - 4r\left[(d-3)Q^3P' + rQ^3P'' - (d-3)QP' - rQP'' - rQ^2P'Q' + 3rP'Q'\right]\Big\},$$

$$\mathcal{L}^{(d+1)} = \frac{r^{d-5}P}{Q^4}\Big\{\alpha_0 r^4 Q^5 - \alpha_1(d-1)r^2Q^2[(d-2)Q(Q^2-1) + 2rQ'] + \alpha_2(d-3)(d-2)(d-1)(Q^2-1)[(d-4)Q(Q^2-1) + 4rQ']\Big\}$$

Spherically symmetric Lagrangian

Case	α_0 α_1 α_2	$P(r)^2$, $Q^2(r)$	Dimension
Einstein–de Sitter	$\neq 0$ $\neq 0$ 0	$P(r)^2 = 1/Q(r)^2 = 1 + \frac{c_1}{r^{d-2}} - \frac{\alpha_0}{\alpha_1 d(d-1)} r^2$	Any
		$P(r)^2 = 1/Q(r)^2 = 1 + \frac{c_1}{r^2} - \frac{\alpha_0}{12\alpha_1} r^2$	5
Pure Gauss–Bonnet	$\neq 0$ 0 $\neq 0$	$P(r)^2 = 1/Q(r)^2 = 1 \pm \frac{1}{r^{d/2-2}}\sqrt{\frac{c_1}{6\alpha_2\binom{d-1}{d-4}} - r^d \frac{\alpha_0}{24\alpha_2\binom{d}{d-4}}}$	Any
		$P(r)^2 = 1/Q(r)^2 = 1 \pm \sqrt{1 + c_1 - \frac{\alpha_0}{24\alpha_2} r^4}$	5
		$P^2(r) = P_0^2\sqrt{48\alpha_2(2c_1+1) \mp 4\sqrt{6}\sqrt{\alpha_2(24\alpha_2 + 96\alpha_2 c_1 - \alpha_0 r^4)} - \alpha_0 r^4}$ $\quad Q^2(r) = \frac{2\left(12\alpha_2 \pm \sqrt{6}\sqrt{\alpha_2(24\alpha_2 + 96\alpha_2 c_1 - \alpha_0 r^4)}\right)}{\alpha_0 r^4 - 96\alpha_2 c_1}$	
	0 0 $\neq 0$	$P(r)^2 = 1/Q(r)^2 = 1 + \frac{c_1}{r^{\frac{d}{2}-2}}$	Any
		Const.	5
Lovelock	$\neq 0$ $\neq 0$ $\neq 0$	$P(r)^2 = 1/Q(r)^2 = 1 \pm \frac{1}{r^{d/2-2}}\sqrt{\frac{c_1}{6\alpha_2\binom{d-1}{d-4}} + r^d\left(\frac{\alpha_1^2}{16\alpha_2^2\binom{d-2}{d-4}^2} - \frac{\alpha_0}{24\alpha_2\binom{d}{d-4}}\right)} - \frac{\alpha_1}{4\alpha_2\binom{d-2}{d-4}} r^2$	Any
		$P(r)^2 = 1/Q(r)^2 = 1 - \frac{\alpha_1 r^2}{4\alpha_2} \pm \frac{\sqrt{3r^4(3\alpha_1^2 - 2\alpha_0\alpha_2) + 6\alpha_2 c_1}}{12\alpha_2}$	5
		$P(r)^2 = P_0^2\sqrt{-4c_1 + \alpha_0 r^4 - 12\alpha_1 r^2}\left[\frac{3\sqrt{r^4 w + 2ux} + \sqrt{3}\left(\alpha_0 x - r^2 w(-3\alpha_1 + z)\right)}{-6\alpha_1 + \alpha_0 r^2 + 2z}\right]^{y/2}\left[\frac{6\alpha_1 - \alpha_0 r^2 + 2z}{3\sqrt{r^4 vw + 2vx} + \sqrt{3}\left(r^2 w(z + 3\alpha_1) + \alpha_0 x\right)}\right]^{s/2}$ $\quad Q(r)^2 = \frac{-3\alpha_1 r^2 + 12\alpha_2 \pm \sqrt{3}\sqrt{8c_1\alpha_2 - 2\alpha_0\alpha_2 r^4 + 3\alpha_1^2 r^4 + 48\alpha_2^2}}{\frac{\alpha_0}{2} r^4 - 6\alpha_1 r^2 - 2c_1}$	
	0 $\neq 0$ $\neq 0$	$P(r)^2 = 1/Q(r)^2 = 1 \pm \frac{1}{r^{d/2-2}}\sqrt{\frac{c_1}{6\alpha_2\binom{d-1}{d-4}} + \frac{\alpha_1^2}{16\alpha_2^2\binom{d-2}{d-4}^2} r^d} - \frac{\alpha_1}{4\alpha_2\binom{d-2}{d-4}} r^2$	Any
		$P(r)^2 = 1/Q(r)^2 = 1 - \frac{\alpha_1 r^2}{4\alpha_2} \pm \frac{\sqrt{9\alpha_1^2 r^4 + 6\alpha_2 c_1}}{12\alpha_2}$	5
		$P(r)^2 = P_0^2\left(2c_1 + \alpha_1 r^2\right)\sqrt{\frac{\sqrt{16\alpha_2(\alpha_2+c_1) + \alpha_1^2 r^4} + \alpha_1 r^2}{8\alpha_2^2 + 2\alpha_2\left(\sqrt{16\alpha_2(\alpha_2+c_1) + \alpha_1^2 r^4} + 4c_1\right) + c_1\left(\sqrt{16\alpha_2(\alpha_2+c_1) + \alpha_1^2 r^4} - \alpha_1 r^2\right)}}$, $\quad Q(r)^2 = \frac{-4\alpha_2 - \sqrt{16\alpha_2(\alpha_2+c_1) + \alpha_1^2 r^4} + \alpha_1 r^2}{4c_1 + 2\alpha_1 r^2}$	
		$P(r)^2 = P_0^2\sqrt{\frac{8\alpha_2^2 + 2\alpha_2\left(\sqrt{16\alpha_2(\alpha_2+c_1) + \alpha_1^2 r^4} + 4c_1\right) + c_1\left(\sqrt{16\alpha_2(\alpha_2+c_1) + \alpha_1^2 r^4} - \alpha_1 r^2\right)}{\sqrt{16\alpha_2(\alpha_2+c_1) + \alpha_1^2 r^4} + \alpha_1 r^2}}$ $\quad Q(r)^2 = \frac{-4\alpha_2 + \sqrt{16\alpha_2(\alpha_2+c_1) + \alpha_1^2 r^4} + \alpha_1 r^2}{4c_1 + 2\alpha_1 r^2}$	
Chern–Simons	$\frac{1}{5l^4}$ $\frac{2}{3l^2}$ 1	$P(r)^2 = 1/Q(r)^2 = 1 - \frac{r^2}{6l^2} \pm \sqrt{\frac{7r^4}{360l^4} + \frac{c_1}{24}}$	
		$P(r)^2 = P_0^2\sqrt{-4c_1 + \frac{r^4}{5l^4} - \frac{8r^2}{l^2}}\left[\frac{\sqrt{3}\left(\frac{r^2}{5l^4} - r^2 w\left(-\frac{2}{l^2} + z\right)\right) + 3\sqrt{u\left(r^4 w + 2x\right)}}{\frac{r^2}{5l^4} - \frac{4}{l^2} + 2z}\right]^{y/2}\left[\frac{-\frac{r^2}{5l^4} + \frac{4}{l^2} + 2z}{\sqrt{3}\left(\frac{r^2}{5l^4} + r^2 w\left(z + \frac{2}{l^2}\right)\right) + 3\sqrt{v\left(r^4 w + 2x\right)}}\right]^{s/2}$ $\quad Q(r)^2 = \frac{\sqrt{24c_1 + \frac{14r^4}{5l^4} + 144} - \frac{2r^2}{l^2} + 12}{-2c_1 + \frac{r^4}{10l^4} - \frac{4r^2}{l^2}}$	

Classical electromagnetism

In coordinates representation

$$S = \int \mathbf{A}\mathrm{d}\mathbf{A} = \int (\partial_\mu A_\nu - \partial_\nu A_\mu) A_p \, dx^\mu \wedge dx^\nu \wedge dx^p = \int \epsilon^{\mu\nu p} F_{\mu\nu} A_p \, d^3x$$

Can be added to the free EM Lagrangian

$$S = \int \left(-\frac{1}{4} F^{\mu\nu} F_{\mu\nu} + \frac{1}{2} m^2 A^\mu A_\mu \right) d^4x$$

By varying with respect to the gauge connection

$$(\Box + m^2)\left(\epsilon_{\alpha\beta\tau} F^{\alpha\beta}\right) = 0 \longrightarrow \textbf{Massive wave equations} \longrightarrow \textbf{Massive photons}$$

Klein-Gordon equation for the vector field $\epsilon_{\alpha\beta\tau} F^{\alpha\beta}$

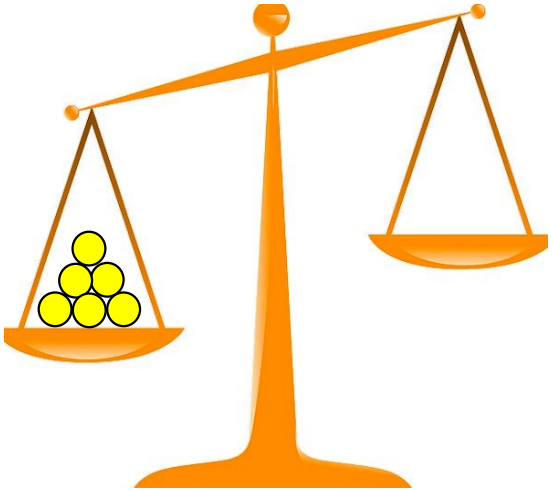

Proca wave equation: $(\Box + m^2) A^\beta = 0 \longrightarrow$ Breaks U(1) invariance

Chern-Simons wave equation: $(\Box + m^2)\left(\epsilon_{\alpha\beta\tau} F^{\alpha\beta}\right) = 0 \longrightarrow$ U(1) invariant, but not conformally invariant

Special relativity is preserved

SU(N) invariant Chern-Simons action and application to biological systems

How to go from this → To this?

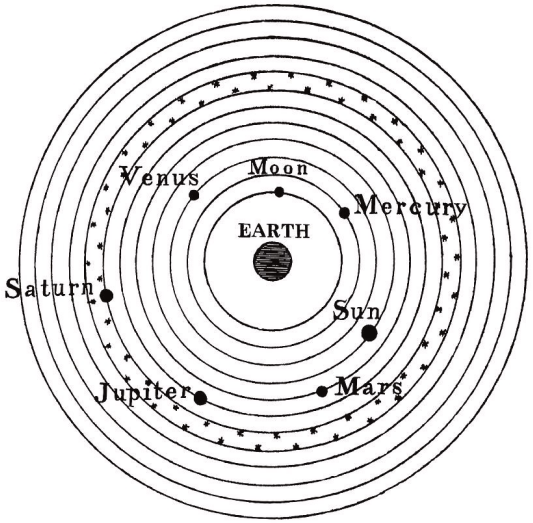

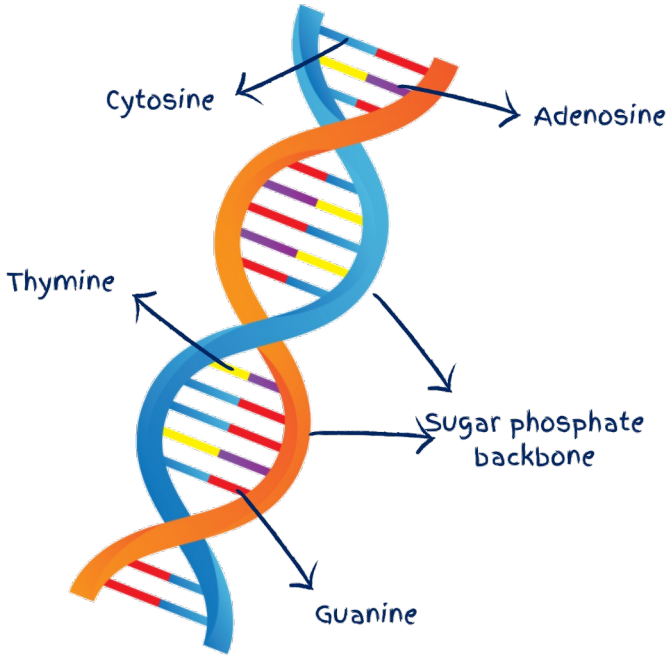


$R_{\mu\nu} - \frac{1}{2} R g_{\mu\nu}$
GRAVITATIONAL BIOLOGY
A CHERN-SIMONS APPROACH TO LIVING SYSTEMS

Main Idea:

The main idea is to deal with the DNA as the space-time, so that the DNA/RNA curvature, can be described in terms of geometry

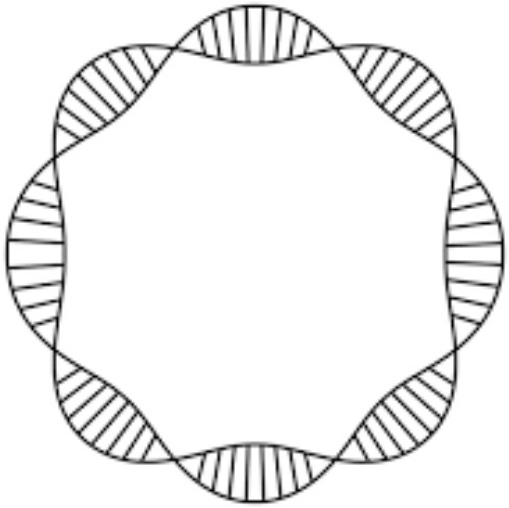

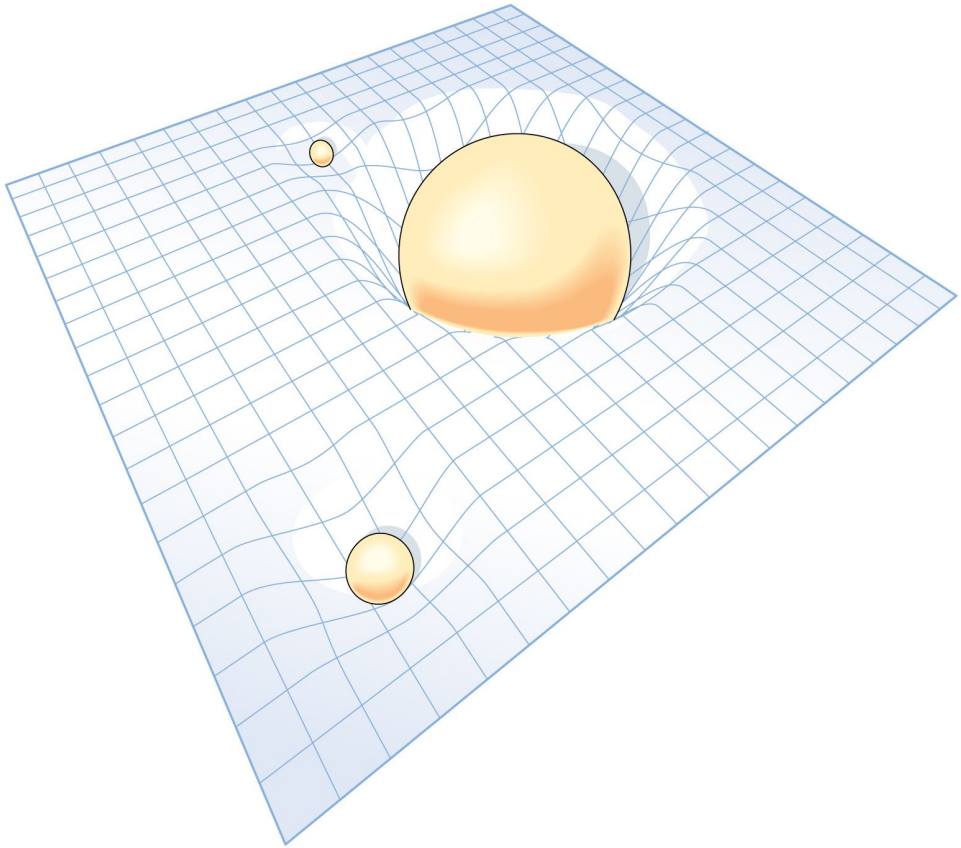

Why is this important?

This is important because the today schematization methods represent one of the most controversial and discussed branches of science

A complete theory capable of predicting the interactions that occur among macro molecules and the corresponding biological implications is still missing

Although the application of Chern-Simons gravity to complex systems seems to be unusual, topological field theories are deeply studied in several branches of physics, besides the application to gravitational interaction.

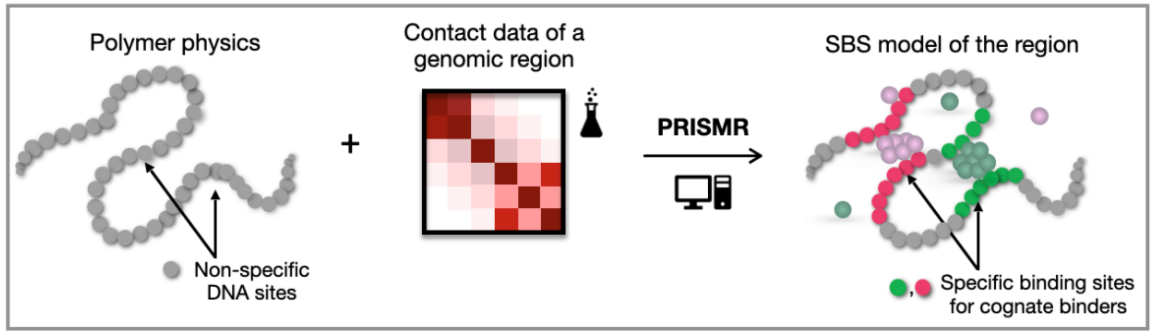

Often it is difficult to reconstruct the DNA shape and figure out whether two or more regions are in contact

Why Chern-Simons?

One may wonder why using the **Chern-Simon theory** to this purpose, instead of considering **General Relativity**

Chern-Simons theory is developed to work in three dimensions (generally, odd dimensions) and it is a good candidate to describe the DNA, which is divided in triplets

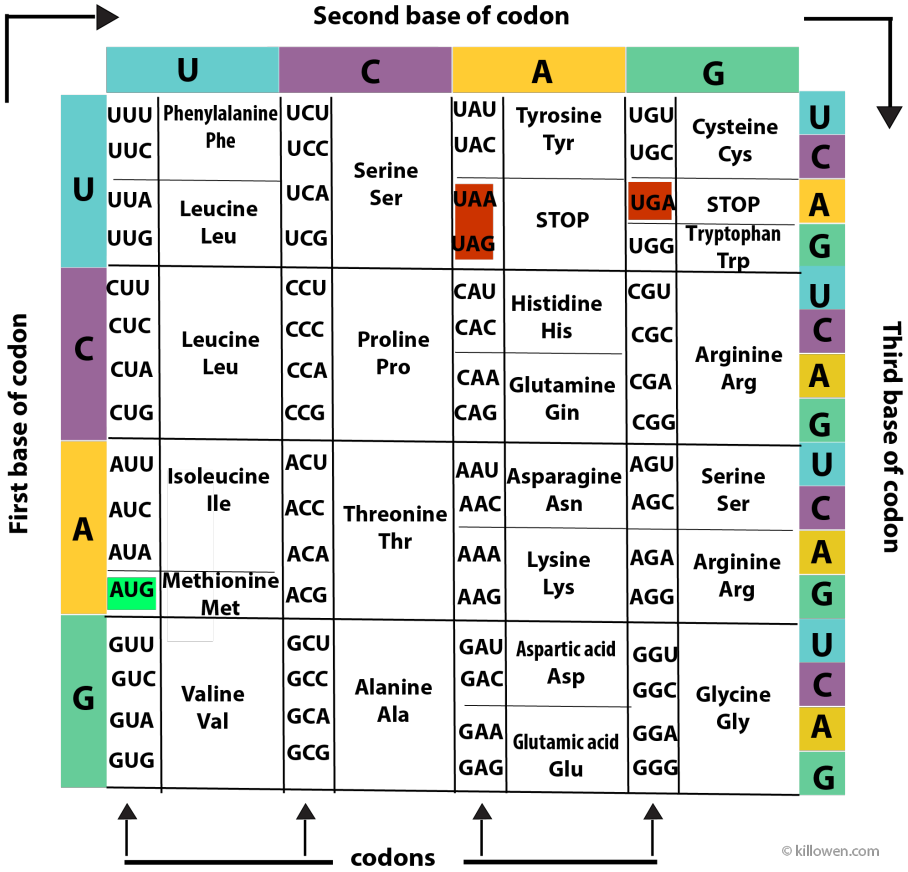

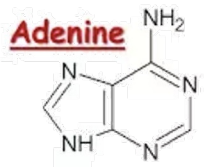

Moreover, CS theory is a topological field theory, which is a key feature to describe the topology of DNA

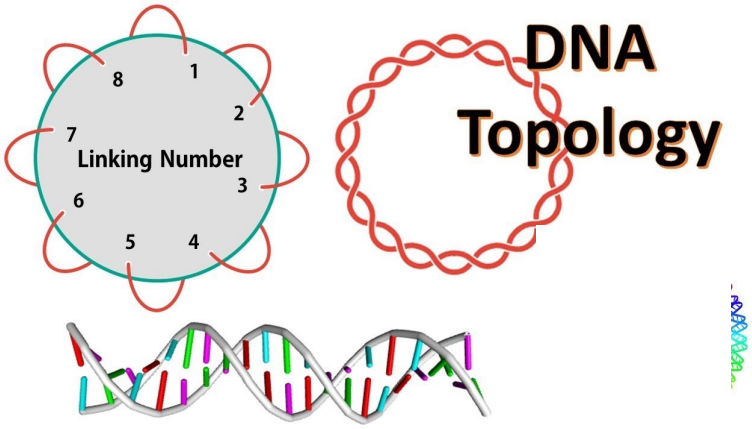

Complex biological systems: the formalism

First step: defining a set of quaternion fields

$$\begin{cases} A_{DNA} := e^{\frac{\pi}{2} i \beta_n} & A_{RNA} := e^{\frac{\pi}{2} j \alpha_n} \\ T_{DNA} := i\, e^{-\frac{\pi}{2} i \beta_n} & U_{RNA} := i\, e^{-\frac{\pi}{2} j \alpha_n} \\ C_{DNA} := j\, e^{i \pi \beta_n} & C_{RNA} := j\, e^{j \pi \alpha_n} \\ G_{DNA} := k\, e^{2 \pi i \beta_n} & G_{RNA} := k\, e^{2 \pi j \alpha_n} \end{cases}$$

$[h] \in \mathbb{H}$: $[h] = a + b\,i + c\,j + d\,k$ and $a, b, c, d \in \mathbb{R}$

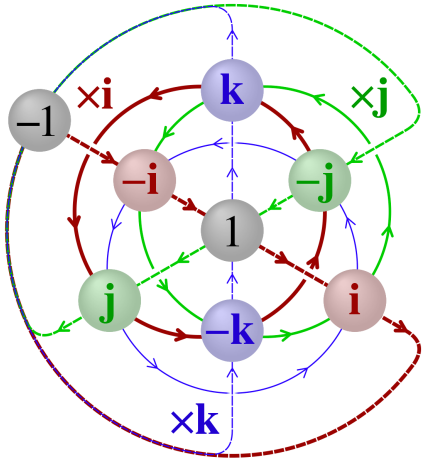

In this way, Chern-Simons currents can be computed for the whole genetic code

In quantum field theory, Wilson loops are **gauge invariant operators** arising from the parallel transport of gauge variables around closed loops.

Considering the SU(2)-invariant Chern-Simon action

$$S^{SU(2)} = \int \mathrm{Tr}\left[\mathbf{A}\mathrm{d}\mathbf{A} + \frac{2}{3}\mathbf{A}\mathbf{A}\mathbf{A}\right]$$

And computing the expectation value of the Wilson Loop

$$W(\mathbf{A}) = \mathrm{tr}\left[\exp\left\{\mathcal{P}\oint \mathbf{A}\right\}\right]$$

$$J = < [W(\mathbf{A})] > = \frac{\int \mathcal{D}A\, e^{iS} \Pi_n W(A_n)}{\int \mathcal{D}A\, e^{iS}}$$

To get the Chern-Simons current J

Amino acid	CS Current	Amino acid	CS Current	Amino acid	CS Current	Amino acid	CS Current
Phe (UUU)	0.7071	Ser (UCU)	0.0534	Tyr (UAU)	0.0214	Cys (UGU)	0.0122
Phe (UUC)	0.5000	Ser (UCC)	0.0495	Tyr (UAC)	0.0205	Cys (UGC)	0.0118
Leu (UUA)	0.3717	Ser (UCA)	0.0460	Sto (UAA)	0.0197	Sto (UGA)	0.0115
Leu (UUG)	0.2887	Ser (UCG)	0.0429	Sto (UAG)	0.0189	Trp (UGG)	0.0112
Leu (CUU)	0.2319	Pro (CCU)	0.0402	His (CAU)	0.0182	Arg (CGU)	0.0109
Leu (CUC)	0.1913	Pro (CCC)	0.0377	His (CAC)	0.0175	Arg (CGC)	0.0106
Leu (CUA)	0.1612	Pro (CCA)	0.0354	Gin (CAA)	0.0169	Arg (CGA)	0.0103
Leu (CUG)	0.1382	Pro (CCG)	0.0334	Gin (CAG)	0.0163	Arg (CGG)	0.0010
Ile (AUU)	0.1201	Thr (ACU)	0.0316	Asn (AAU)	0.0157	Ser (AGU)	0.0098
Ile (AUC)	0.1057	Thr (ACC)	0.0299	Asn (AAC)	0.0152	Ser (AGC)	0.0096
Ile (AUA)	0.0939	Thr (ACA)	0.0284	Lys (AAA)	0.0147	Arg (AGA)	0.0093
Met (AUG)	0.0841	Thr (ACG)	0.0270	Lys (AAG)	0.0142	Arg (AGG)	0.0091
Val (GUU)	0.0759	Ala (GCU)	0.0257	Asp (GAU)	0.0138	Gly (GGU)	0.0089
Val (GUC)	0.0690	Ala (GCC)	0.0245	Asp (GAC)	0.0134	Gly (GGC)	0.0087
Val (GUA)	0.0630	Ala (GCA)	0.0234	Glu (GAA)	0.0129	Gly (GGA)	0.0085
Val (GUG)	0.0579	Ala (GCG)	0.0224	Glu (GAG)	0.0126	Gly (GGG)	0.0083

S. Capozziello, R. Pincak, K. Kanjamapornkul and E. N. Saridakis. Annalen Phys 530 (2018), 1700271

Chern-Simons current: *provides an indication about the point-like curvature of a given sequence*

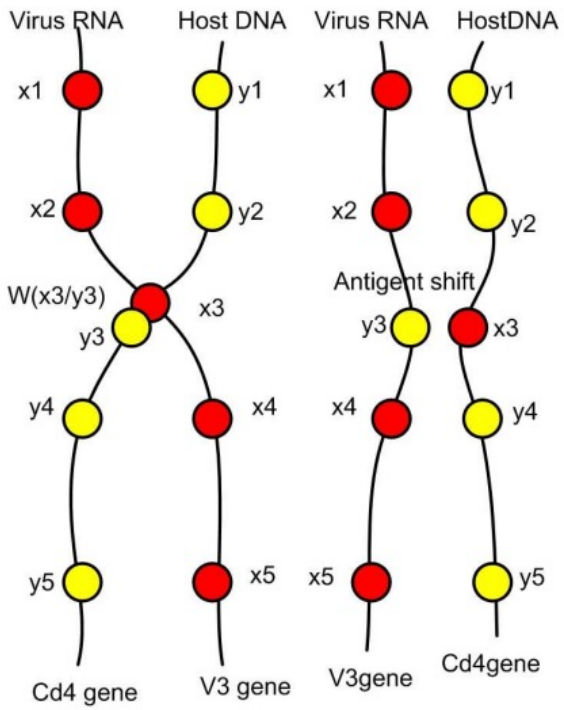

Each point is labeled by a different current

The approach:

1) Introduce mutations of amino acids
2) Study the effects of the mutations

What we expect

We theoretically expect the mutation to level out the curvature spectrum, providing smoother variations of the current with respect to the original sequence. In analogy with other physical systems, the curved point is surrounded by a non-equilibrium region, which in turn tends to mutate in order to reach a minimum free energy state.

In agreement with ***Gibbs free energy*** minimization $\Delta\mathcal{G} < 0$

$$\mathcal{G} = U - TS + pV$$

Can be assumed to be constants

Potential energy

*S. Capozziello, R. Pincak, K. Kanjamapornkul and E. N. Saridakis. Annalen Phys **530** (2018), 1700271*

By means of the Nitrogen bases, it is possible to define different possible ”real” states

$$[s_1] = ([A], [T]^*) \in T_p\mathcal{M}, \quad [p1] = [s_1]^* = [s_{11}]^* = ([A], [T]^*)^* \in T_p^*\mathcal{M}$$

$$[s_2] = ([A], [NA]) \in T_p\mathcal{M}, \quad [s_2]^* = ([A], [NA])^* \in T_p^*\mathcal{M}$$

$$[s_3] = ([C], [G]^*) \in T_p\mathcal{M}, \quad [s_3]^* = ([C], [G]^*)^* \in T_p^*\mathcal{M}$$

$$[s_4] = ([C], [NC]) \in T_p\mathcal{M}, \quad [s_4]^* = ([C], [NC])^* \in T_p^*\mathcal{M}$$

$$[s_5] = ([T], [T]^*) \in T_p\mathcal{M}, \quad [s_5]^* = ([T], [T]^*)^* \in T_p^*\mathcal{M}$$

$$[s_6] = ([T], [NA]) \in T_p\mathcal{M}, \quad [s_6]^* = ([T], [NA])^* \in T_p^*\mathcal{M}$$

$$[s_7] = ([G], [G]^*) \in T_p\mathcal{M}, \quad [s_7]^* = ([G], [G]^*)^* \in T_p\mathcal{M}$$

$$[s_8] = ([G], [NC]) \in T_p\mathcal{M}, \quad [s_8]^* = ([G], [NC])^* \in T_p\mathcal{M}.$$

64 states of codon and anti-states of codon state

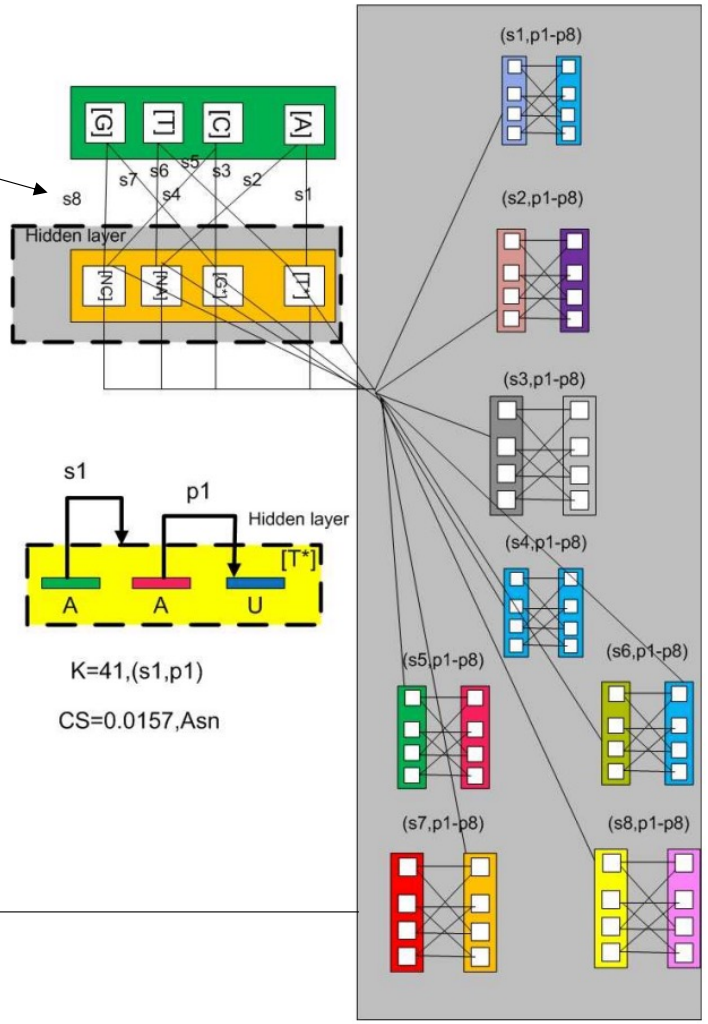

$$\Gamma_{ij}^k = \frac{1}{2} g^{kl}(\partial_j g_{jk} + \partial_i g_{jk} - \partial_k g_{jk}), \qquad \nabla_g\, g = 0.$$

To Compute the States we impose:
- No torsion
- Metric Compatibility

Not all possible combinations actually result in real states, but only a few of them

Each first alpha alphabet of [si] states contain substate of p-orbital of spinor field in codon.

$$\begin{cases} A_{DNA} := e^{\frac{\pi}{2} i\beta_n} & A_{RNA} := e^{\frac{\pi}{2} j\alpha_n} \\ T_{DNA} := i\, e^{-\frac{\pi}{2} i\beta_n} & U_{RNA} := i\, e^{-\frac{\pi}{2} j\alpha_n} \\ C_{DNA} := j\, e^{i\pi\beta_n} & C_{RNA} := j\, e^{j\pi\alpha_n} \\ G_{DNA} := k\, e^{2\pi i\beta_n} & G_{RNA} := k\, e^{2\pi j\alpha_n} \end{cases}$$

$$W(\mathbf{A}) = \mathrm{tr}\left[\exp\left\{\mathcal{P}\oint \mathbf{A}\right\}\right]$$

$$J =< [W(\mathbf{A})] >= \frac{\int \mathcal{D}A\, e^{iS} \Pi_n W(A_n)}{\int \mathcal{D}A\, e^{iS}}$$

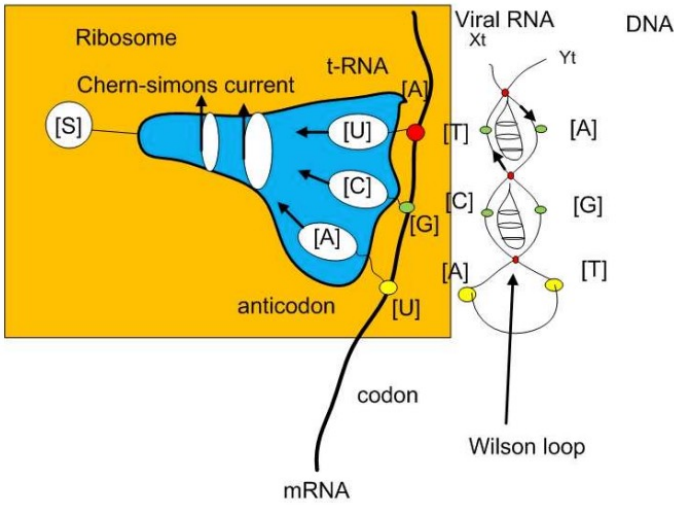

The expectation value of the Wilson Loop, which in turn is defined using the Nitrogen bases, provides the Chern-Simons current, capable of describing the DNA/RNA curvature using the same formalism as the gravitational interaction

---

On the left, the interaction of retrotranspon can be visualized as the entanglement state in the loop space of time series data with extradimension over the Hopf fibration

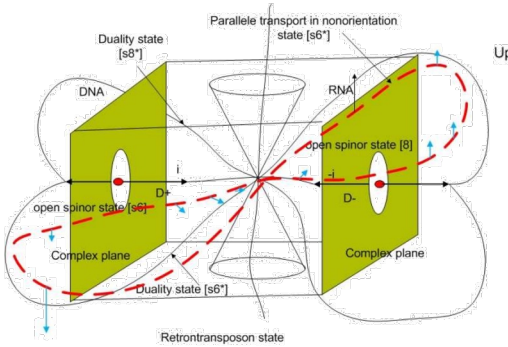

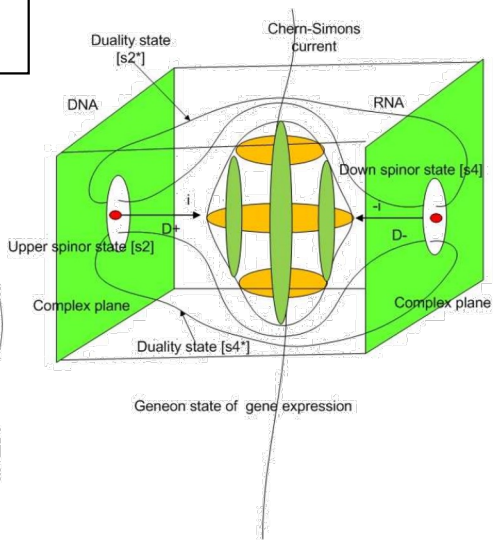

orientation area of fiber space of DNA, it is an active part of the state with spherical shape of a single histone protein in the active zone of DNA, that is the 2% area of gene expression in the human genome. We notice that the induced Chern-Simons current in this area is quantized into separeted fiber in the covering space of the sphere.

This formalism can be also used to describe docking between molecules

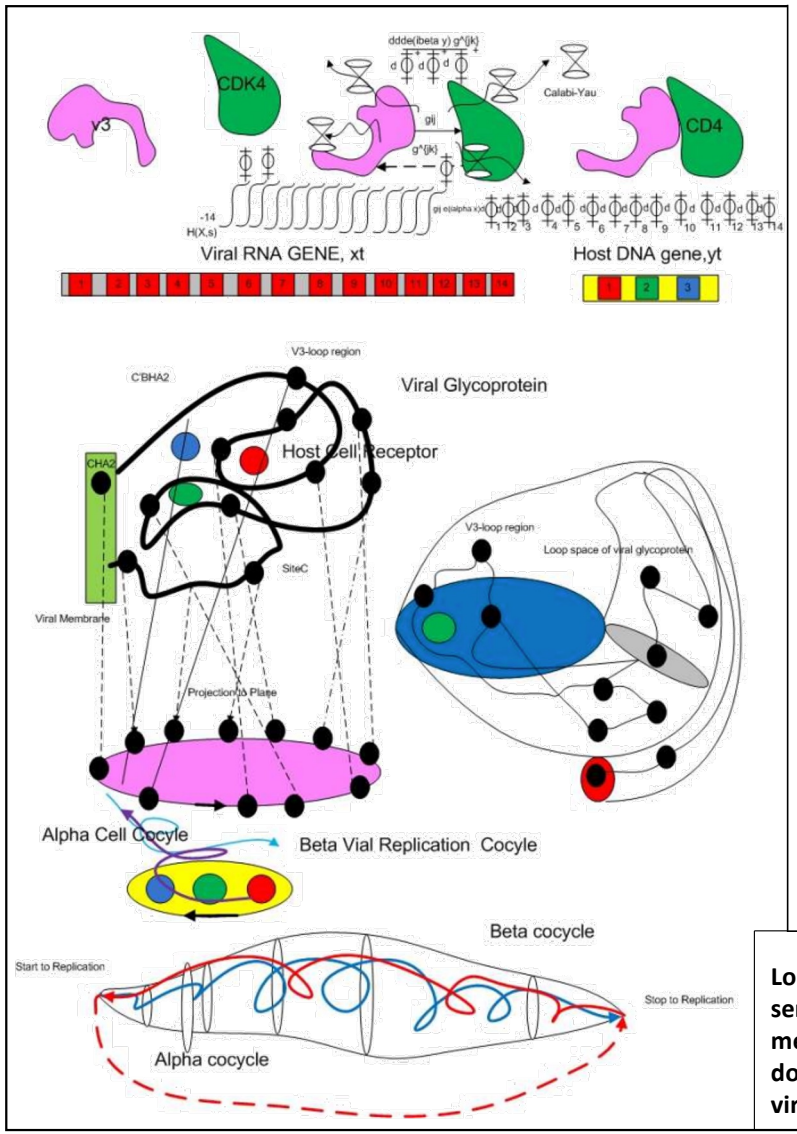

Loop space of time series data over cell membrane and docking state when a virus attaches a cell

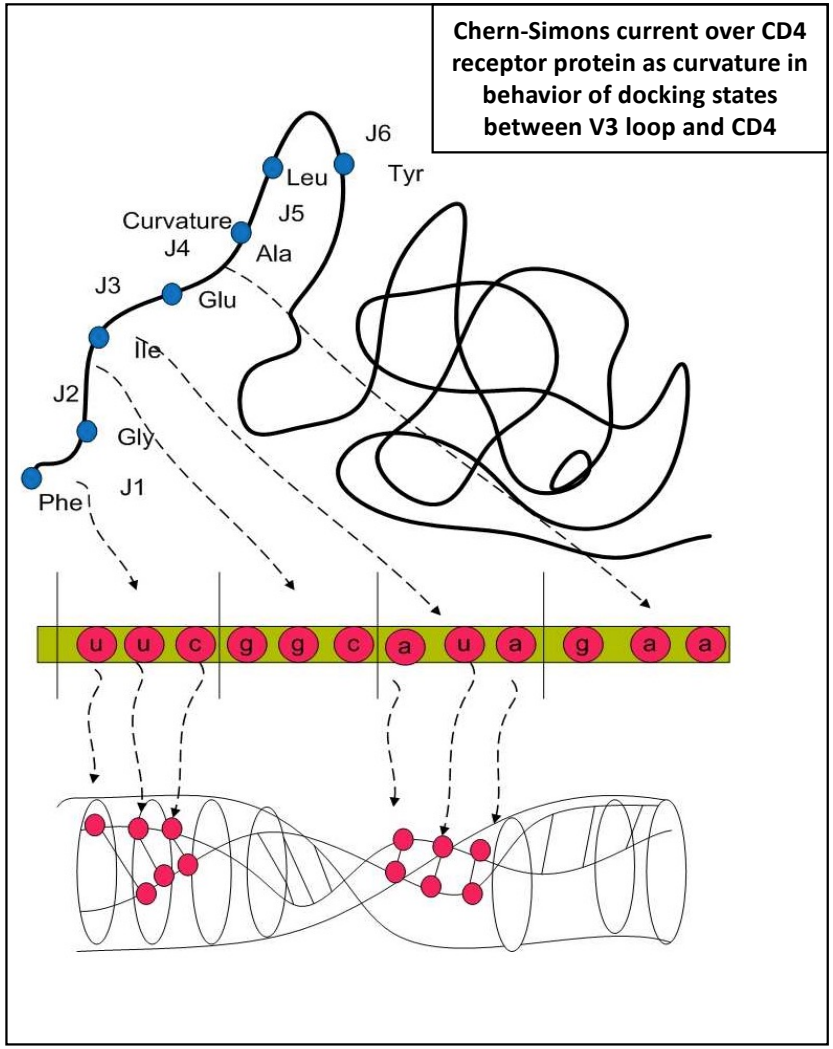

Chern-Simons current over CD4 receptor protein as curvature in behavior of docking states between V3 loop and CD4

For instance, the equation of glycoprotein attached to the CD4 T-host cell is given by

$$adj\begin{bmatrix} D\Phi_1(x_t) & 0 & 0 & 0\,0\,0 & 0 & 0 & 0 & 0 \\ 0 & D\Phi_2(x_t) & 0 & 0\,0\,0 & 0 & 0 & 0 & 0 \\ 0 & 0 & \cdots & 0\,0\,0 & 0 & 0 & 0 & 0 \\ 0 & 0 & 0 & 0\,0\,0 & D\Phi_{14}(x_t) & 0 & 0 & 0 \\ 0 & 0 & 0 & 0\,0\,0 & 0 & d\Phi_1^+(y_t) & 0 & 0 \\ 0 & 0 & 0 & 0\,0\,0 & 0 & 0 & d\Phi_2^+(y_t) & 0 \\ 0 & 0 & 0 & 0\,0\,0 & 0 & 0 & 0 & d\Phi_3^+(y_t) \end{bmatrix}$$

$$= adj_{y_t} x_t = \{y_t, x_t\} = 0.$$

with

$$D\Phi_k(x_k), k = 1, 2, \cdots 14 = \frac{d}{dS^{-1}} \int_{S^{-1}}^{\Phi_k} g_{kk} e^{-j2\pi\beta_k(x_k)} d\beta_k := \frac{d}{d\beta_k} \int_{S^{-1}}^{\Phi_k} g_{kk} e^{-2\pi j \beta_i(x_k)} d\beta_k$$

$$d\Phi_p^+(y_t), p = 1, 2, 3 = \frac{d}{dS^1} g^{pp} \Phi_p^+(y_t) = \frac{g^{pp} de^{2\pi i \alpha_p(y_p)}}{d\alpha_p}$$

14 bases for ghost fields, 3 bases for anti-ghost fields

The table below shows the definition of first 14-ghost fields in E8 × E8 model of artificial HIV viral v3 loop and cd4 as a supermanifold structure

Ghost field Φ_i	site name	moduli state space variable	Anti-Ghost field Φ_i^+	site name	moduli state space variable
Φ_1	C	x_t	Φ_1^+	CD4 receptor	y_t
Φ_2	N	x_t	Φ_2^+	CXCR4 coreceptor	y_t
Φ_3	α_1	x_t	Φ_3^+	CCR5 coreceptor	y_t
Φ_4	L_A	x_t			
Φ_5	α_5	x_t			
Φ_6	L_C	x_t			
Φ_7	α_3	x_t			
Φ_8	L_E	x_t			
Φ_9	V5	x_t			
Φ_{10}	V4	x_t			
Φ_{11}	V3	x_t			
Φ_{12}	V1/V2	x_t			
Φ_{13}	Bridging Sheet	x_t			
Φ_{14}	β Sheet	x_t			

The picture shows the **duality** in plane while the virus attaches the surface of cell membrane with the same curvature and with different curvature. **On the left side,** it is demonstrated the homotopy equivalent state of **protein-protein interaction with different curvature while docking**. The remaining area between docking curvature is not zero. This area can induce a contractible to new 14-extradimensions by using the homotopy equivalent map. When we take the cohomology group to that surface, the computation of cohomology is not zero. This fact is implying a nonequilibrium state of docking between V3 loop HIV virus and host cell receptor CD4 in difference curvature. On the right hand situation of docking state, there is an equilibrium state with the same curvature. The rest of the area between docking can be contractible to a point and the cohomology group is zero.

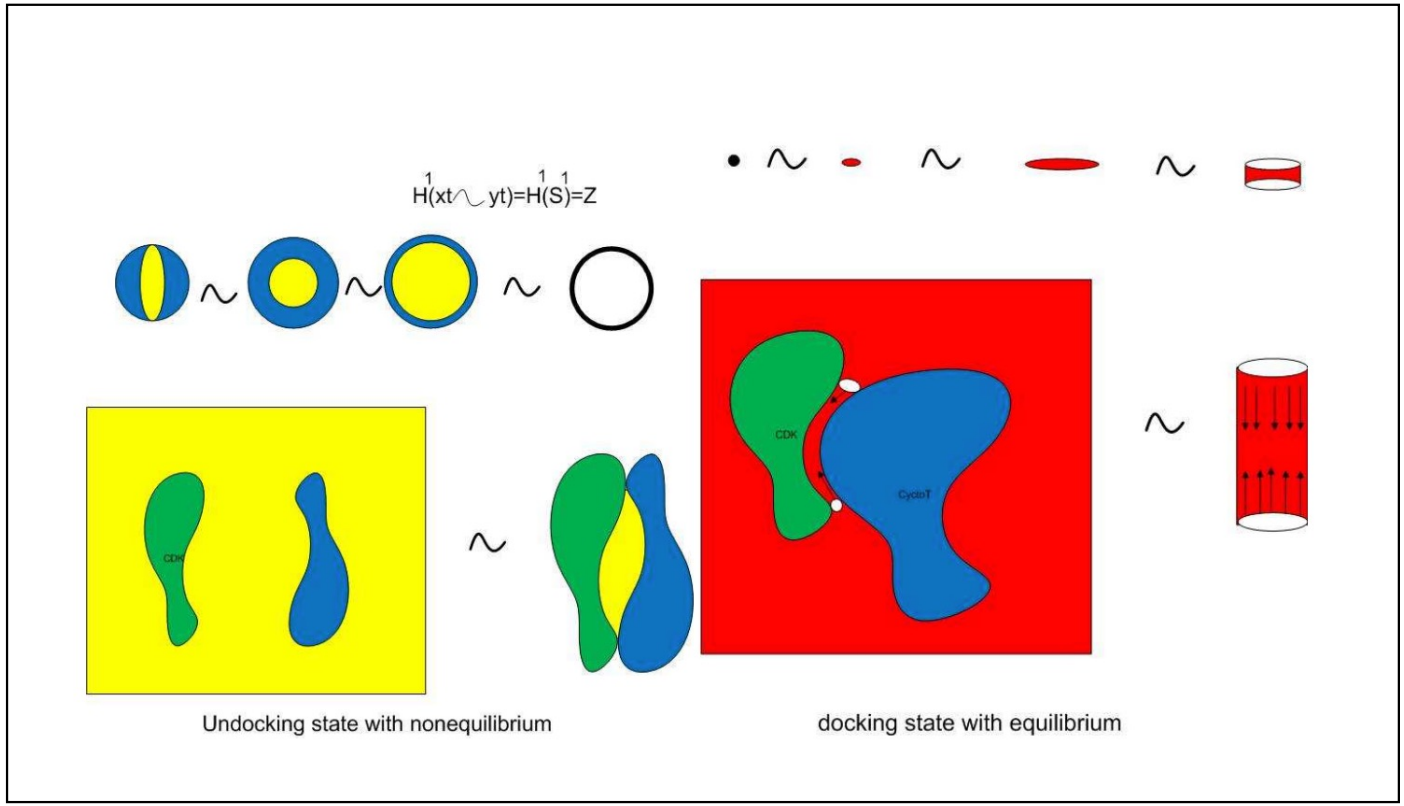

What about the "Junk" area?

Junk DNA is a part of DNA that does not directly code for proteins, but still plays an important role in regulating gene expression and in the structure of the genome.

In the past, this DNA was thought to be useless

Recent research has shown that it performs crucial functions, such as producing non-coding RNAs (ncRNAs) that regulate the expression of other genes.

2%

Genes

98%

Trash

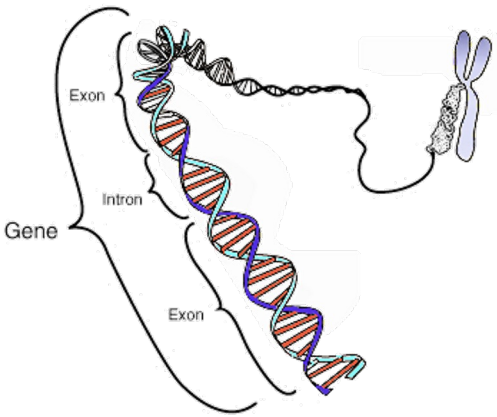

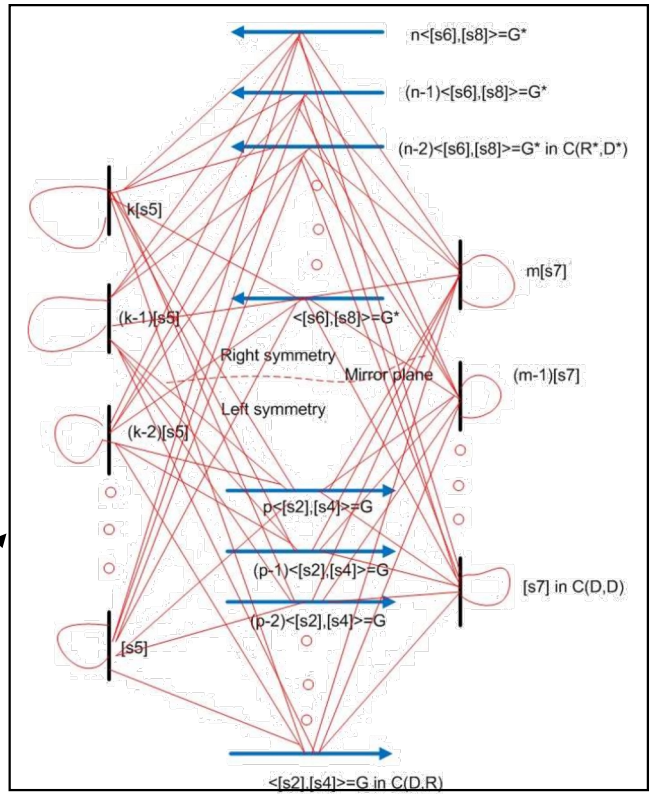

The transition state in trash DNA between transposon, retrotransposon and active gene in the moduli-state space Diophantine equation. The transitions have active and passive layer. The active layer is in the active genes while the passive layer is in the area of trash DNA. The transition between states and hidden states of these 2 layers satisfies the moduli -state space Diophantine equation. The modulo makes the gene expression into circle and in fiber of the transition state.

In our formalism, trash DNA is rapresented by hidden states, which can be related to «real states»

Computationally, it is thus possible to deffine a new Chern-Simons current for hidden states

$$|\varphi^{geneon}_{[A_i,s_i,\mu]}>=\oint_{H^2(X;D,R)}\Pi_\mu W_\mu\frac{1}{([s^*]-[s_2])([s^*]-[s_4])}d[s_2]\wedge d[s_4]$$

$$|\varphi^{anti-geneon}_{[A_i,s_i,\mu]}>=\oint_{H^2(X;D,D)}\Pi_\mu W_\mu\frac{1}{([s^*]-[s_1])([s^*]-[s_3])}d[s_1]\wedge d[s_3]$$

$$|\varphi^{transponson}_{[A_i,s_i^*,\mu]}>=\oint_{H^2(X;D^*,D^*)}\Pi_\mu W_\mu\frac{1}{([s^*]-[s_5])([s^*]-[s_7])}d[s_5]\wedge d[s_7]$$

$$|\varphi^{retrotransponson}_{[A_i,s_i^*,\mu]}>=\oint_{H^2(X;D^*,D^*)}\Pi_\mu W_\mu\frac{1}{([s^*]-[s_6])([s^*]-[s_8])}d[s_6]\wedge d[s_8]$$

with

$$[s_1]=([A],[T]^*)\in T_p\mathcal{M},\quad [p1]=[s_1]^*=[s_{11}]^*=([A],[T]^*)^*\in T_p^*\mathcal{M}$$

$$[s_2]=([A],[NA])\in T_p\mathcal{M},\quad [s_2]^*=([A],[NA])^*\in T_p^*\mathcal{M}$$

$$[s_3]=([C],[G]^*)\in T_p\mathcal{M},\quad [s_3]^*=([C],[G]^*)^*\in T_p^*\mathcal{M}$$

$$[s_4]=([C],[NC])\in T_p\mathcal{M},\quad [s_4]^*=([C],[NC])^*\in T_p^*\mathcal{M}$$

$$[s_5]=([T],[T]^*)\in T_p\mathcal{M},\quad [s_5]^*=([T],[T]^*)^*\in T_p^*\mathcal{M}$$

$$[s_6]=([T],[NA])\in T_p\mathcal{M},\quad [s_6]^*=([T],[NA])^*\in T_p^*\mathcal{M}$$

$$[s_7]=([G],[G]^*)\in T_p\mathcal{M},\quad [s_7]^*=([G],[G]^*)^*\in T_p\mathcal{M}$$

$$[s_8]=([G],[NC])\in T_p\mathcal{M},\quad [s_8]^*=([G],[NC])^*\in T_p\mathcal{M}.$$

First, one has to define new states starting from the «real states»

Then, the CS current reads

$$J^{\mu=k}=\int trH^3(\mathcal{M}):=\frac{k}{4\pi}\int_{H^3(D.R.P)}A\partial A+\frac{2}{3}A\wedge A\wedge A$$

$$J(K,q)=\sum_{i=1}^{n}a_nq^n:=\oint_{H^n(\mathcal{O}_\mathcal{X})}W_{D^+}\frac{1}{(\Pi_i([s]-[s_i])}d[]s.$$

For instance, for retrotrasposon it becomes

$$J^{k=retrotransposon}=J^{k=\beta_i}=-i\sqrt{\frac{2}{28-\frac{2}{\beta_i}}}\sin\frac{\pi}{28-\frac{2}{\beta_i}}$$

In so doing, the trash DNA is described at the same level as “standard” DNA

Application to KRAS and SARS-CoV2

The **KRAS gene (Kirsten Rat Sarcoma Virus)** is an oncogene that, when mutated, can contribute to the development of cancer. It is involved in cell signaling and the regulation of cell growth and proliferation. KRAS mutations are common in several types of cancer, such as lung, colorectal, and pancreatic cancer.

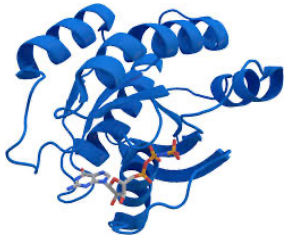

The **SARS-CoV-2 (Severe Acute Respiratory Syndrome COronaVirus 2)** previously named 2019 novel coronavirus (2019-nCoV), is a viral strain of the species Betacoronavirus pandemicum belonging to the genus Betacoronavirus (family Coronaviridae), subgenus Sarbecovirus, discovered around the end of 2019; it is the seventh coronavirus known to infect humans.

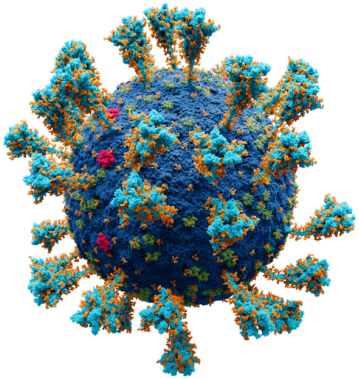

Approach:

1) We consider the Chern-Simons Current of series of amino acids in KRAS gene
2) We introduce known mutations in the original sequence
3) We compute the variation of the Chern-Simons current

Result:

1) The induced mutation yields variations in terms of curvature
2) The amount of variation can suggest the probability or frequency of the mutation, as well as its impact in the gene

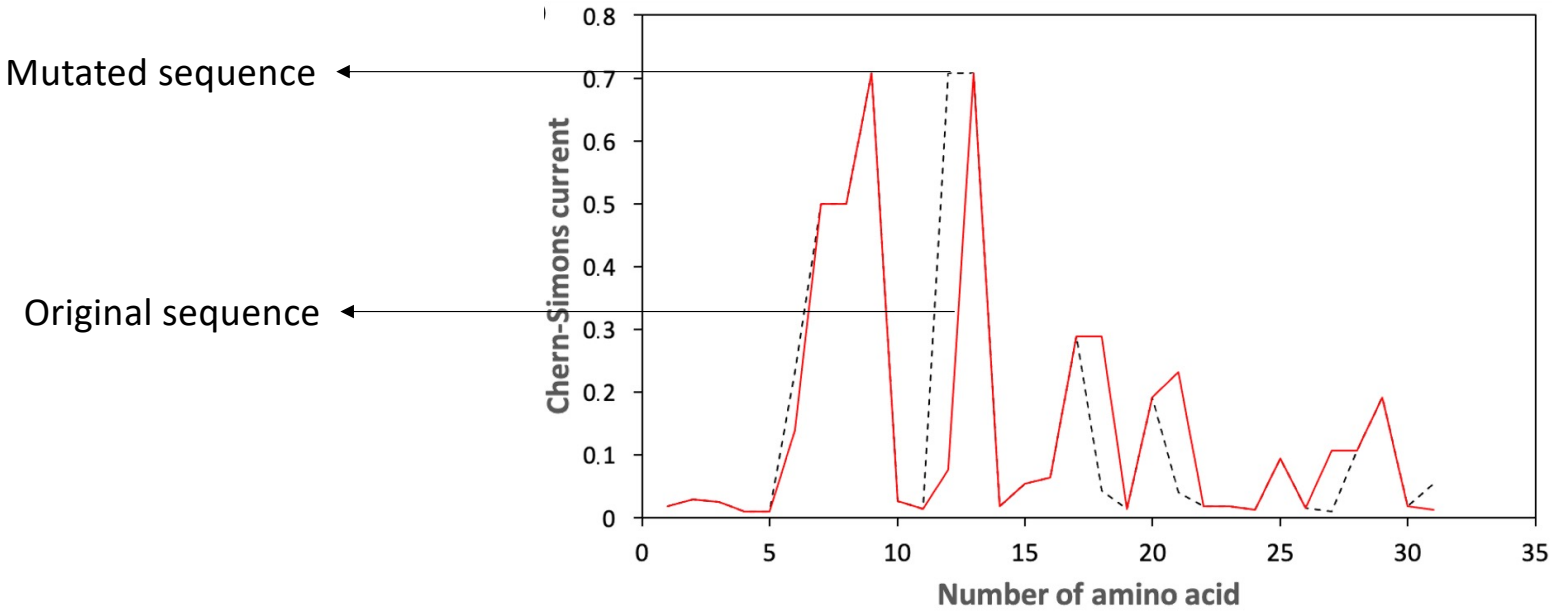

In detail: application to KRAS human gene

Position	Ref. Base	Mutation	Ref. Amino	Mutation	Current Variation (%)	Initial CS current	Mutated CS current
25,215,485	CUU	CUG	L	L	-40.405	0.2319	0.1382
25,215,501	UUU	GUU	F	V	-89.266	0.7071	0.0759
25,215,520	UCG	UUG	S	L	572.96	0.0429	0.2887
25,215,529	CCU	CUU	P	L	476.866	0.0402	0.2319
25,215,539	UGU	UGC	C	C	-3.279	0.0122	0.0118
25,215,547	AGC	AUC	S	I	1001.042	0.0096	0.1057
25,215,559	UCU	UGU	S	C	-77.154	0.0534	0.0122

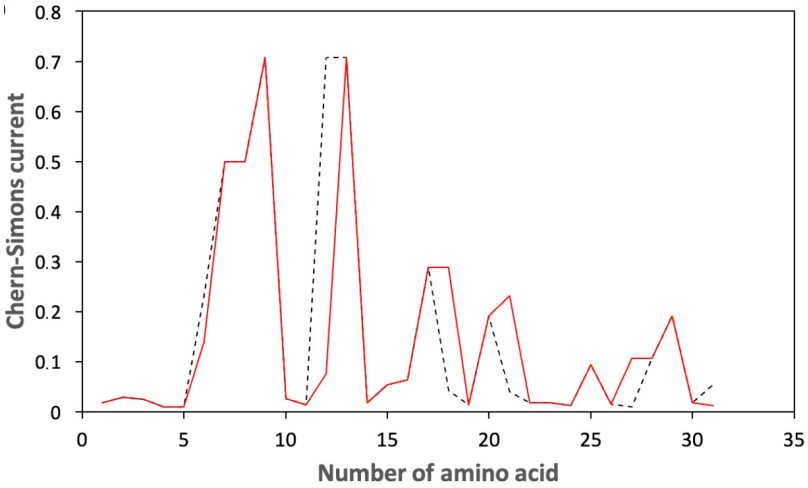

Figures show the comparison between the original sequence (black dashed line) and the mutated one (red solid line)

Position	Ref. Base	Mutation	Ref. Amino	Mutation	Current Variation (%)	Initial CS current	Mutated CS current
25,245,294	UUC	UUG	F	L	-42.26	0.5	0.2887
25,245,314	AAU	AUU	N	I	664.968	0.0157	0.1201
25,245,321	CUG	CUU	L	L	67.8	0.1382	0.2319
25,245,332	GGC	GAC	G	D	54.023	0.0087	0.0134
25,245,338	CUU	CCU	L	P	-82.665	0.2319	0.0402
25,245,350	ACC	AAC	T	N	-49.164	0.0299	0.0152
25,245,365	CAC	CCC	H	P	115.429	0.0175	0.0377
25,245,370	UUU	GUU	F	V	-89.266	0.7071	0.0759
25,245,378	UUC	UUU	F	F	41.42	0.5	0.7071

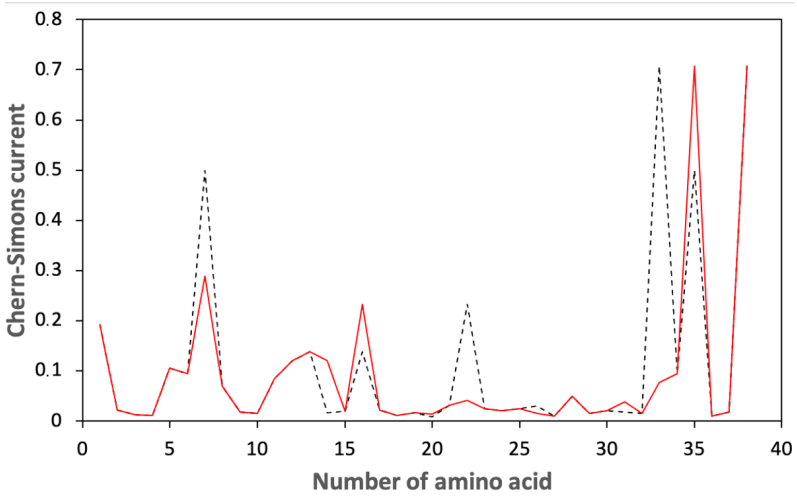

F. Bajardi, S. Capozziello et al. *Eur.Phys.J.Plus* 136 (2021) 10, 1080

Application to KRAS human gene

Position	Ref. Base	Mutation	Ref. Amino	Mutation	Current Variation (%)	Initial CS current	Mutated CS current
25,245,279	UAU	UAA	Y	Stop	-7.944	0.0214	0.0197
25,245,294	UUC	UUG	F	L	-42.260	0.5	0.2887
25,245,314	AAU	AUU	N	I	664.968	0.0157	0.1201
25,245,332	GGC	GAC	G	D	54.023	0.0087	0.0134
25,245,342	GCC	GCU	A	A	4.898	0.0245	0.0257
25,245,350	ACC	AAC	T	N	-49.164	0.0299	0.0152
25,245,365	CAC	CCC	H	P	115.429	0.0175	0.0377
25,245,370	UUU	AUU	F	I	-83.015	0.7071	0.1201

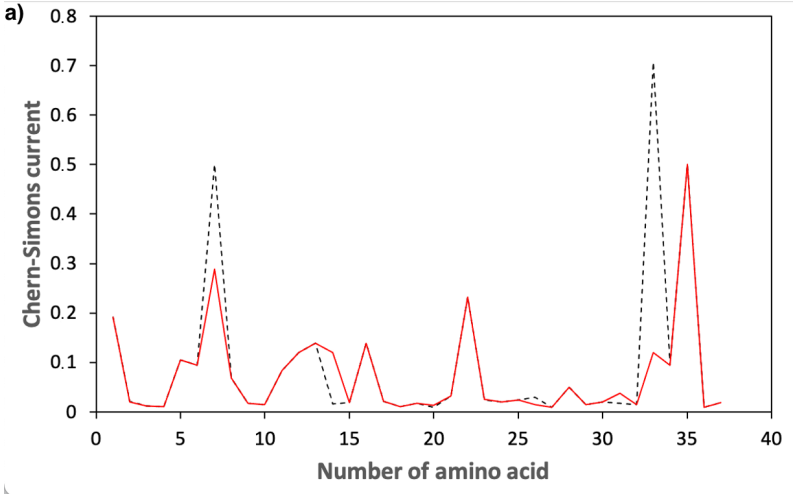

Figures show the comparison between the original sequence (black dashed line) and the mutated one (red solid line)

Position	Ref. Base	Mutation	Ref. Amino	Mutation	Current Variation (%)	Initial CS current	Mutated CS current
25,245,294	UUC	UUG	F	L	-42.26	0.5	0.2887
25,245,314	AAU	AUU	N	I	664.968	0.0157	0.1201
25,245,321	CUG	CUU	L	L	67.8	0.1382	0.2319
25,245,332	GGC	GAC	G	D	54.023	0.0087	0.0134
25,245,338	CUU	CCU	L	P	-82.665	0.2319	0.0402
25,245,350	ACC	AAC	T	N	-49.164	0.0299	0.0152
25,245,365	CAC	CCC	H	P	115.429	0.0175	0.0377
25,245,370	UUU	GUU	F	V	-89.266	0.7071	0.0759
25,245,378	UUC	UUU	F	F	41.42	0.5	0.7071

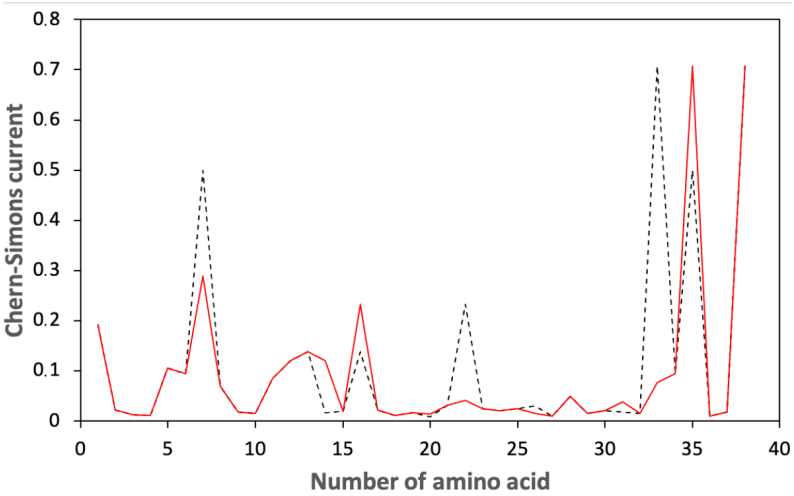

Application to SARS-CoV-2 virus: second approach

$$\text{Variation } (\%)_2 = \frac{j_n - j_{n-1}}{j_{n-1}}$$

20C Mutations				
Position	20C Triplet	20C Current	Variation (%) with respect to previous position	Variation (%) with respect to subsequent position
220	CTG	0.1382	717	-90
555	ACT	0.0316	145	-19
810	ACA	0.0284	-55	-46
1323	ACA	0.0284	-20	-53
1656	AAG	0.0142	-3	-21
1978	CCC	0.0377	33	42
2047	CCA	0.0354	141	95
2130	GTT	0.0759	195	0
2454	GTT	0.0759	522	-79
2597	AAT	0.0157	-79	72
3353	***CTT***	0.2319	1533	-94
3354	AAG	0.0142	-94	435
3378	GTG	0.0579	26	542
3451	GAC	0.0134	-82	-32
4236	AAC	0.0152	-96	0
5168	TAG	0.0189	-73	-41
5475	GTA	0.063	-25	358
6054	***CTA***	0.1612	821	-42
6092	TTG	0.2887	3004	-93
6098	ATA	0.0939	62	-81
6129	CTG	0.1382	931	-93
6161	ATG	0.0841	-30	-37
6398	CGT	0.0109	-93	478
6773	TTA	0.3717	2518	-57
7118	CTT	0.2319	1377	-88
7167	GCT	0.0257	41	265
7180	GAT	0.0138	-98	10
7315	GAT	0.0138	27	1286
7331	ATA	0.0939	165	-91
7517	AAG	0.0142	67	746
7584	***GAA***	0.0129	-83	-31
7601	AAT	0.0157	-50	-43
7620	GCA	0.0234	29	51
7801	GCA	0.0234	163	-45
8437	CTA	0.1612	-30	-91
8548	CAG	0.0163	-93	255
8549	***GTG***	0.0579	255	45
8556	TTT	0.7071	339	-80
8732	CTG	0.1382	-72	-24
8897	GAT	0.0138	13	191
9234	***GTC***	0.069	143	22
9331	CAT	0.0182	-97	786
9404	CCT	0.0402	-92	-74
9542	ACT	0.0316	272	69
9536	***CCA***	0.0354	12	-75
9809	AGT	0.0098	-91	491

19A Mutations				
Position	19A Triplet	19A Current	Variation (%) with respect to previous position	Variation (%) with respect to subsequent position
925	TTC	0.5	836	-96
2840	***AGC***	0.0096	6213	70
3607	TTT	0.7071	0	-97
3840	AAA	0.0147	-97	1201
4716	***CTA***	0.1612	821	-90
5829	CTG	0.1382	362	68
5866	ATG	0.0841	436	-62
5933	TCT	0.0534	299	596
7714	***GAT***	0.0138	-15	450
8847	CAG	0.0163	-37	889
9294	TTT	0.7071	412	-96
9697	TAT	0.0214	-9	-31
9762	TAC	0.0205	53	39

20B Mutations				
Position	20B Triplet	20B Current	Variation (%) with respect to previous position	Variation (%) with respect to subsequent position
217	TCC	0.0495	-83	-74
301	***ATT***	0.1201	1191	-91
1002	ACT	0.0316	0	280
1247	***ACT***	0.0316	145	-55
1306	AAG	0.0142	-3	81
1668	ATT	0.1201	125	-88
1709	GCT	0.0257	0	-41
1908	TTC	0.5	2236	-94
2148	AAC	0.0152	-93	-3
2231	ATA	0.0939	-22	28
2426	***ACT***	0.0316	11	280
3279	***GGT***	0.0089	-29	37
3892	TGT	0.0122	-28	466
4425	***ACA***	0.0284	33	-71
4805	***CCG***	0.0334	120	89
4993	ACA	0.0284	0	-57
5006	***ACC***	0.0299	-84	1143
5305	CTT	0.2319	717	-93
5462	***CGC***	0.0106	-28	334
5785	AGC	0.0096	-90	3772
6098	***ACA***	0.0284	-51	-38
6299	ATT	0.1201	586	15
6479	TCA	0.046	-71	708
6590	CTC	0.1913	127	-67
7120	ACC	0.0299	5	-69
7170	GTC	0.069	279	-23
7577	***AGC***	0.0096	8	196
7601	***AAT***	0.0157	-50	-43
7670	GCT	0.0257	-79	-48
7713	***CAG***	0.0163	-24	-45
7781	CCT	0.0402	-25	-75
7816	ACA	0.0284	-25	-45
7823	***ACC***	0.0299	-61	-5
8036	GAT	0.0138	-19	233
8081	CTT	0.2319	119	-80
8082	TCA	0.046	-80	-76
8218	GAC	0.0134	-53	13
9237	TCA	0.046	124	-38
9262	TAG	0.0189	97	-22
9283	GTA	0.063	37	-71
9516	GGT	0.0089	2	10
9571	ATG	0.0841	472	-37

20A Mutations				
Position	20A Triplet	20A Current	Variation (%) with respect to previous position	Variation (%) with respect to subsequent position
61	GTT	0.0759	772	280
266	***ACC***	0.0299	123	1572
2008	ACC	0.0299	90	-63
2130	GCT	0.0257	0	195
3840	AAG	0.0142	-97	1247
6098	ACA	0.0284	-51	-38
6161	ACG	0.027	-78	98
6590	CCC	0.0377	-55	67
6773	TGA	0.0115	-19	1302
6800	CTA	0.1612	927	-57
6998	CGT	0.0109	-87	67
7069	TGA	0.0115	-88	6049
7322	***GCT***	0.0257	-40	1346
8036	GAC	0.0134	-21	243
8434	***AGA***	0.0093	-98	141
8437	CCA	0.0354	-85	-58
8847	CAG	0.0163	-51	1179
9516	GGC	0.0087	0	13
9540	***AGG***	0.0091	-7	272
9546	AGA	0.0093	-64	804
9557	GCT	0.0257	-89	1023
9708	GAC	0.0134	-6	10
9795	GTA	0.063	273	-78

Only four sequences have been considered for this analysis, since they are the only ones generating variants

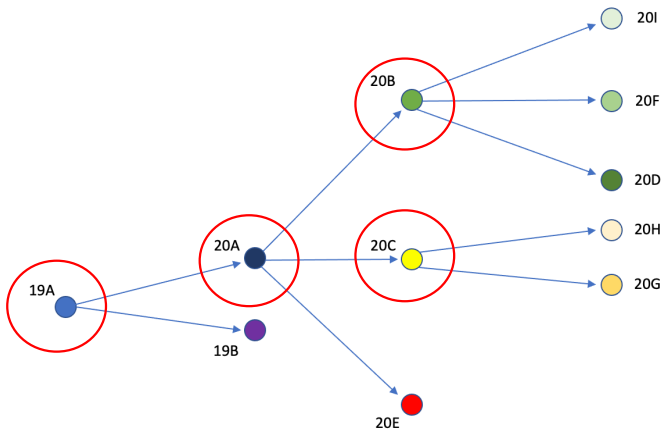

Application to SARS-CoV-2 virus: first approach

$$\text{Slope} = \frac{\text{Mutated Seq.} - \text{Original Seq.}}{\text{Original Seq.}}$$

Position	20C Triplet	20C Current	20G Triplet	20G Current	Current Variation (%)
220	CTG	0.1382	TTG	0.2887	109
555	ACT	0.0316	ACC	0.0299	-5
1323	ACA	0.0284	ACC	0.0299	5
1978	CCC	0.0377	CCT	0.0402	7
2130	GTT	0.0759	GCT	0.0257	-66
3353	***CTT***	0.2319	***TTT***	0.7071	205
4236	AAC	0.0152	AAT	0.0157	3
5168	TAG	0.0189	TAT	0.0214	13
6054	***CTA***	0.1612	***CTG***	0.1382	-14
6092	TTG	0.2887	TTT	0.7071	145
6098	ATA	0.0939	ACA	0.0284	-70
6129	CTG	0.1382	TTG	0.2887	109
6161	ATG	0.0841	ACG	0.027	-68
6773	TTA	0.3717	TGA	0.0115	-97
7331	ATA	0.0939	ATT	0.1201	28
7620	GCA	0.0234	TCA	0.046	97
8437	CTA	0.1612	CCA	0.0354	-78
8549	***GTG***	0.0579	***TTG***	0.2887	399
8556	TTT	0.7071	TTC	0.5	-29
8897	GAT	0.0138	TAT	0.0214	55
9234	***GTC***	0.069	***GTT***	0.0759	10
9404	CCT	0.0402	TCT	0.0534	33
9536	***CCA***	0.0354	***CTA***	0.1612	355
9726	***CAG***	0.0163	***CTG***	0.1382	748

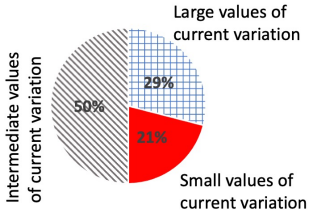

Position	20B Triplet	20B Current	20I Triplet	20I Current	Current Variation (%)
217	TCC	0.0495	TCT	0.0534	8
1002	ACT	0.0316	ATT	0.1201	280
1668	ATT	0.1201	ATA	0.0939	-22
1709	GCT	0.0257	GAT	0.0138	-46
1908	TTC	0.5	TTT	0.7071	41
2231	ATA	0.0939	ACA	0.0284	-70
4805	***CCG***	0.0334	***CTG***	0.1382	314
5006	***ACC***	0.0299	***ATC***	0.1057	254
5305	CTT	0.2319	CCT	0.0402	-83
5785	AGC	0.0096	GGC	0.0087	-9
6590	CTC	0.1913	CCC	0.0377	-80
7170	GTC	0.069	ATC	0.1057	53
7601	***AAT***	0.0157	***TAT***	0.0214	36
7670	GCT	0.0257	GAT	0.0138	-46
7781	CCT	0.0402	CAT	0.0182	-55
7816	ACA	0.0284	ATA	0.0939	231
8036	GAT	0.0138	GAC	0.0134	-3
8082	TCA	0.046	GCA	0.0234	-49
8218	GAC	0.0134	CAC	0.0175	31
9237	TCA	0.046	TTA	0.3717	708
9262	TAG	0.0189	TAT	0.0214	13
9283	GTA	0.063	GTG	0.0579	-8

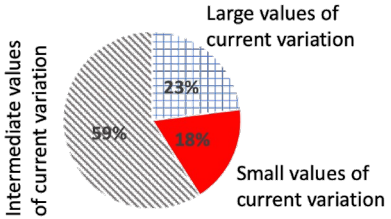

Position	20B Triplet	20B Current	20F Triplet	20F Current	Current Variation (%)
301	***ATT***	0.1201	***TTT***	0.7071	489
2426	***ACT***	0.0316	***ACC***	0.0299	-5
5462	***CGC***	0.0106	***CTC***	0.1913	1705
6098	***ACA***	0.0284	***ATA***	0.0939	231
6590	CTC	0.1913	CCC	0.0377	-80
7577	***AGC***	0.0096	***AAC***	0.0152	58
7713	***CAG***	0.0163	***CAA***	0.0169	4
8036	GAT	0.0138	GAC	0.0134	-3
9516	GGT	0.0089	GGC	0.0087	-2

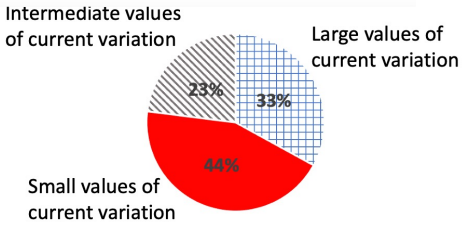

Position	20B Triplet	20B Current	20D Triplet	20D Current	Current Variation (%)
1247	***ACT***	0.0316	***ATT***	0.1201	280
1306	AAG	0.0142	AAT	0.0157	11
2148	AAC	0.0152	AAT	0.0157	3
3279	***GGT***	0.0089	***AGT***	0.0098	10
3892	TGT	0.0122	TGC	0.0118	-3
4425	***ACA***	0.0284	***ATA***	0.0939	231
4993	ACA	0.0284	ATA	0.0939	231
6299	ATT	0.1201	ACT	0.0316	-74
6479	TCA	0.046	TCG	0.0429	-7
6590	CTC	0.1913	CCC	0.0377	-80
7120	ACC	0.0299	ATC	0.1057	254
7823	***ACC***	0.0299	***ACT***	0.0316	6
8036	GAT	0.0138	GAC	0.0134	-3
8081	CTT	0.2319	CTC	0.1913	-18
9516	GGT	0.0089	GGC	0.0087	-2
9571	ATG	0.0841	ATT	0.1201	43

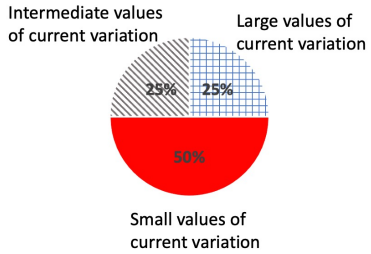

Position	20A Triplet	20A Current	20E Triplet	20E Current	Current Variation (%)
61	GTT	0.0759	GTC	0.069	-9
2008	ACC	0.0299	ACT	0.0316	6
3840	AAG	0.0142	AAA	0.0147	4
6800	CTA	0.1612	CCA	0.0354	-78
6998	CGT	0.0109	CCT	0.0402	269
7069	TGA	0.0115	TTA	0.3717	3132
7322	***GCT***	0.0257	***GTT***	0.0759	195
9546	AGA	0.0093	AAA	0.0147	58
9557	GCT	0.0257	GTT	0.0759	195
9708	GAC	0.0134	GAT	0.0138	3
9795	GTA	0.063	TTA	0.3717	490

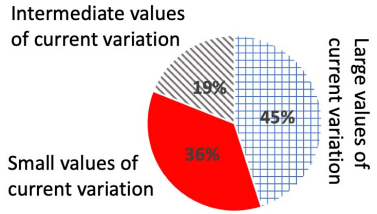

Position	20C Triplet	20C Current	20H Triplet	20H Current	Current Variation (%)
810	ACA	0.0284	ACT	0.0316	11
1656	AAG	0.0142	AAT	0.0157	11
2047	CCA	0.0354	CTA	0.1612	355
2130	GTT	0.0759	GCT	0.0257	-66
2454	GTT	0.0759	GTC	0.069	-9
2597	AAT	0.0157	AGT	0.0098	-38
3354	AAG	0.0142	AGG	0.0091	-36
3378	GTG	0.0579	GTT	0.0759	31
3451	GAC	0.0134	GAT	0.0138	3
5475	GTA	0.063	GTG	0.0579	-8
6098	ATA	0.0939	ACA	0.0284	-70
6161	ATG	0.0841	ACG	0.027	-68
6398	CGT	0.0109	CAT	0.0182	67
6773	TTA	0.3717	TGA	0.0115	-97
7118	CTT	0.2319	TTT	0.7071	205
7167	GCT	0.0257	GTT	0.0759	195
7180	GAT	0.0138	GCT	0.0257	86
7315	GAT	0.0138	GGT	0.0089	-36
7517	AAG	0.0142	AAT	0.0157	11
7584	***GAA***	0.0129	***AAA***	0.0147	14
7601	***AAT***	0.0157	***TAT***	0.0214	36
7801	GCA	0.0234	GTA	0.063	169
8437	CTA	0.1612	CCA	0.0354	-78
8548	CAG	0.0163	TAG	0.0189	16
8732	CTG	0.1382	TTG	0.2887	109
9331	CAT	0.0182	TAT	0.0214	18
9542	ACT	0.0316	ATT	0.1201	280
9809	AGT	0.0098	ATT	0.1201	1126

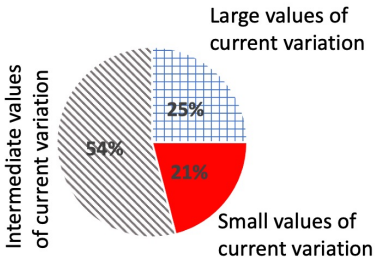

Application to SARS-CoV-2 virus: first approach

Result:

The one-to-one comparison between the original and the corresponding mutated sequences shows that 60% of mutations corresponds to extreme values of current. Such percentage increases up to 80% if we consider only those mutations which will effectively spread out

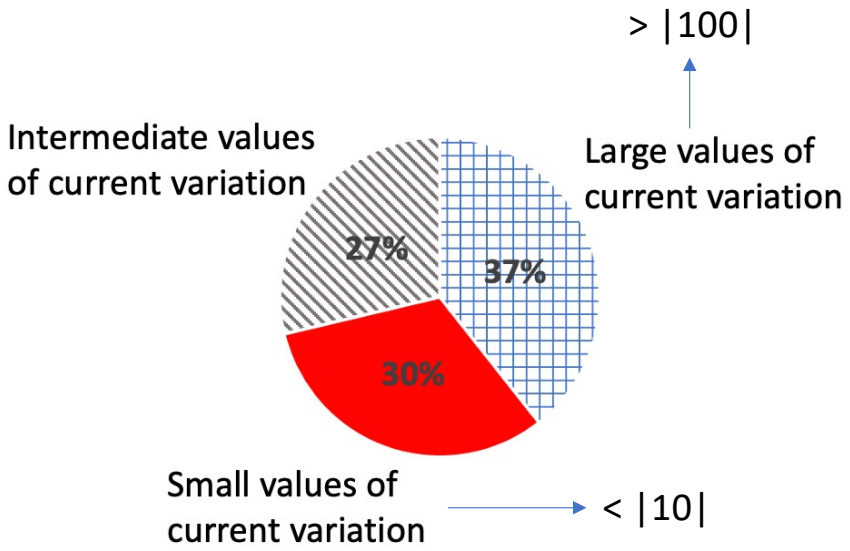

This statistic can be used to point out which occurred mutation of the sequence can be more likely to evolve in a real, spread out variant of the virus. Once we know the position of a given mutation, Chern–Simons currents can allow to predict which type of triplets will arise from such mutation

However, no information regarding the mutation position can be provided

Results

The analysis again shows that mutations mostly occur where the current variation is high-valued. More precisely, in a set of 125 total mutations, 59% of them (74/125) are located in points where the curvature undergoes abrupt variations. This percentage increases up to 69%, if only noticeable mutations which had more impact in the development of the corresponding variants are considered.

Physical interpretation

This result can be explained based on the achievements of the previous section, where non- equilibrium points turned out to be best candidates to provide nitrogen bases mutations. More precisely, large values of the current variations account for peaked regions, which tend to evolve to a lower curvature, that is a lower current. Reversing the argument, large variations of current are exhibited by points which are far from the minimum of energy, which is supposed to occur where the trend is constant.

Conclusions and perspectives: Chern-Simons gravity to biological systems

Theoretical Perspectives

1. *Extend Lovelock gravity*
2. *Study other topological theories towards biological systems*

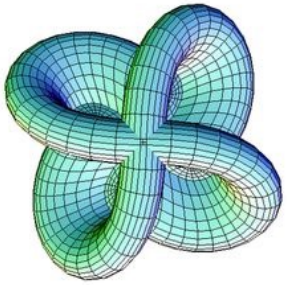

Applications

1. *Focus on other part of DNA*
2. *Compare with other DNA schematization methods*
3. *Understand the link between CS current and disease*

A Supersymmetry and Quantum Cryptosystem with Path Integral Approach in Biology
Salvatore Capozziello, Richard Pincak, Erik Bartos
DOI: 10.3390/sym12081214
Published in: Symmetry 12 (2020) 8, 1214

Chern-Simons Current of Left and Right Chiral Superspace in Graphene Wormhole
Salvatore Capozziello , Richard Pincak, Erik Bartos
DOI: 10.3390/sym12050774
Published in: Symmetry 12 (2020) 5, 774

The Chern-Simons current in time series of knots and links in proteins
Salvatore Capozziello, Richard Pincak
DOI: 10.1016/j.aop.2018.04.002
Published in: Annals Phys. 393 (2018), 413-446

The Chern-Simons Current in Systems of DNA-RNA Transcriptions
Salvatore Capozziello, Richard Pincak, Kabin Kanjamapornkul, Emmanuel N. Saridakis
DOI: 10.1002/andp.201700271
Published in: Annalen Phys. 530 (2018) 4, 1700271

Anomaly on Superspace of Time Series Data
Salvatore Capozziello, Richard Pincak, Kabin Kanjamapornkul
DOI: 10.1515/zna-2017-0274
Published in: Z.Naturforsch.A 72 (2017) 12, 1077-1091

Further related papers

| R. Benedetti, F. Bajardi, S. Capozziello, V. Carafa, M. Conte, M. R. Del Sorbo, A. Nebbioso, M. Singh, H. G. Stunnenberg and M. Valadan, *et al.* "Different approaches to unveil biomolecule configurations and their mutual interactions," 10.1080/00032719.2020.1716241, [arXiv:2002.02364 [q-bio.BM]].

] F. Bajardi, C. Altucci, L.Altucci, R. Benedetti, S. Capozziello, M. Del Sorbo and G. Franci, "DNA Mutations via Chern-Simons Current," (2021) 2021.06.22.449396v1

F. Bajardi, D. Vernieri, S. Capozziello, "Exact solutions in higher-dimensional Lovelock and AdS5 Chern-Simons gravity," 10.1088/1475-7516/2021/11/057